Hebert III, L. 2023. Allometric and metabolic scaling: arguments for design...and clues to explaining pre-flood longevity? In J.H. Whitmore (editor), *Proceedings of the Ninth International Conference on Creationism*, pp. 206-227. Cedarville, Ohio: Cedarville University International Conference on Creationism.

CEDARVILLE UNIVERSITY

9th ICC 2023

ALLOMETRIC AND METABOLIC SCALING: ARGUMENTS FOR DESIGN... AND CLUES TO EXPLAINING PRE-FLOOD LONGEVITY?

Leo (Jake) Hebert III, Institute for Creation Research, P.O. Box 59029 Dallas, Texas 75229 USA, jhebert@ICR.org

ABSTRACT

Among creationists and intelligent design theorists, there is much interest in developing a theory of biological design. Evolutionary scientists have made much progress in this area by assuming living things are designed for efficiency, despite the obvious logical incongruity in their reasoning. This area of research is closely connected to the field of allometry, the study of how different parts of an organism grow or scale in relation to the size of the organism as a whole. The allometric metabolic scaling theory of physicist Geoffrey West and biologists Brian Enquist and John Brown (WBE theory) assumes living things are constructed to efficiently deliver nutrients to their constituent cells. It uses this assumption to successfully predict features of avian and mammalian circulatory and respiratory systems. Moreover, their ontogenetic extension of the theory provides a theoretical justification for the sigmoid mass-versus-age growth curves exhibited by many living creatures. It also provides a general mathematical expression for an organism's age at maturity. Numerous empirical studies have demonstrated a positive correlation between ages at maturity (first reproduction and/or skeletal maturity) and total lifespan: the higher the age at maturity, the longer an organism's lifespan. This link to empirical observations may ultimately enable the WBE theory (or one like it) to help explain the large sizes of many pre-Flood creatures, as well as the extreme longevity of the pre-Flood and immediate post-Flood patriarchs. Indeed, fossil data and paleo-ontogenetic growth curves, already published in the mainstream evolutionary literature, provide at least five lines of possible evidence that some animals were experiencing much greater longevity in the pre-Flood and immediate post-Flood worlds, just as humans were. Because of the potential significance of this information to the creation community, this paper also discusses these lines of evidence, while recognizing their preliminary nature and the need for further research before making a strong claim in this regard.

KEYWORDS

Metabolic scaling, allometry, longevity, scaling laws, WBE theory, optimization, design, giantism

I. INTRODUCTION

Creationists have long maintained, in agreement with Scripture (Romans 1:20), that evidence of design in living things is overwhelming, and increased understanding of biological systems will strengthen that argument. Within the creationist and intelligent design communities, there is increased interest in applying engineering principles to the understanding of living things (Guliuzza 2017, Miller 2022). Because engineers attempt to maximize certain product features (durability, efficiency, etc.) while minimizing others (cost of production, amount of material used, etc.), one would expect living things, if designed, to show evidence of intentionally optimized features. Although evolutionary biologists acknowledge that living things seem well-designed, they refuse to acknowledge an intelligent Designer. Dawkins (1986) essentially argues that the appearance of design is an illusion, and Ayala (2007) states that Darwin's greatest discovery was explaining design without a Designer.

How then do evolutionists account for the origin of optimized features that in any realm other than evolutionary biology would reasonably be understood as a product of engineering, especially since organisms possess these traits in abundance? They claim that highly engineered qualities like efficiency, optimization, robustness, etc. that typically characterize non-random living systems were produced by a random trial-and-error process where (Godfrey-Smith 2015, pp. 18-20) "natural selection has continually honed" organisms. This "tinkering" process is the "mechanism that is at the very core of any living system and that has been refined over millions of years" (Jacob 1977, p. 1165). Clearly, evolutionists deal with the obvious teleology demonstrated in optimized features by personifying nature with a God-like selective agency to "hone" and "refine" a primitive arrangement of molecules into a complicated, optimized system. But this leaves one wondering, how does this faith-based mantra pervading the evolutionary literature about nature "honing" and "refining" organisms differ in its metaphysical makeup from another scientist's explanation that biological optimization is the product of an intelligent Creator?

Despite this obvious logical inconsistency in their position, evolutionary biologists have long recognized that biological characteristics are, in some sense, optimal, and they have devised mechanistic theories to explain this optimization from basic physical principles. Ideally, such

optimization theories would be generally applicable, even over the enormous size range exhibited by living things (Figure 1).

II. ALLOMETRY AND ITS IMPORTANCE TO CREATION RESEARCHERS

A. Overview

Biophysical optimization is closely linked to allometry, the study of how biological characteristics vary with size in relation to the size of the organism as a whole. As an organism grows, different body parts may grow at different rates. Allometry involves the study of body part sizes as well as temporal characteristics such as heart rate and life span. Allometric relationships are usually expressed in the mathematical form

$$Y = Y_0 X^{\lambda} \tag{1}$$

where Y is some biological characteristic, X is some body measurement (total body mass, limb length, etc.), Y_0 is a normalization constant, and λ is an exponent, often some multiple of ¼. The fact that integer multiples of ¼ appear so often in allometric equations has been a long-standing puzzle (Brown et al. 2000). Linear graphs are often used to express allometric relationships, since a power-law function plots as a straight line on a log-log graph.

There is a long history of allometric studies going back at least as far as Galileo Galilei, who noted that increasing the linear dimensions of an object by a factor n will cause the object's surface area to become n^2 times larger, but its volume to become n^3 times larger (Galilei 1638). Leonardo da Vinci (Minamino and Tateno 2014) observed that the cross sectional area of a tree below a branch point is equal to the sums of the cross-sectional areas above that branch point. A.-G. Greenhill (1881) published a short derivation of the maximum height to which a tree of given proportions could grow without buckling under its own weight. In the 20th century, mathematical biologist D'Arcy Thompson published his book *On Growth and Form* (1917), which used basic mathematics to describe the shapes and growth of living things. Evolutionary geneticist J. B. S. Haldane (1927) observed that physical constraints placed limits on the sizes of organisms. The term allometry was coined in 1936 in a joint paper by Julian Huxley and Georges Teissier (1936), based upon Huxley's work in studying growth rates of fiddler crabs (Huxley 1924).

Allometry is of interest to creationists for several reasons. Allometric relationships are often used to estimate the sizes of extinct creatures, especially when an entire skeleton is unavailable (Seebacher 2001). Also, creationists have long suggested that unusual anatomical features of ancient humans may somehow be related to extreme longevity. Cuozzo (1998a) suggested that allometric changes in craniofacial features of people who have lived in excess of one hundred years could be responsible for the heavy brow ridges and lower facial heights seen in Neanderthal skulls. A possible problem with this explanation is that a few extant humans have very thick brow ridges, even at younger ages (Rupe and Sanford 2017, Tomkins 2019). Line (2013) suggested that ancient humans may have had robust, thick bones as a necessary engineering constraint for great longevity, rather than the robustness being the result of longevity *per se*. The robustness in the bones of even Neanderthal children and adolescents (Lubenow 2004) would seem to be consistent with Line's suggestion. Since a discussion of these differences in the skeletons of ancient humans falls within the domain of allometry, it is worthwhile for creationist paleontologists to be familiar with the subject, especially since evolutionary scientists could misinterpret allometric differences between extinct and extant forms as degrees of evolutionary development between those forms. Finally, it is possible to mathematically derive allometric relationships by assuming that the engineering principles of optimization and efficiency will be characteristics of living things, especially with regard to energy consumption. Such relationships are *prima facie* evidence for the design of living things.

B. Kleiber's Law

Agricultural scientists Max Kleiber and Samuel Brody independently obtained an important empirical allometric relationship. They concluded in Kleiber (1932, 1947, 1961), Brody et al. (1932), and Brody (1945) that for warm-blooded animals like birds or domesticated cattle, the animal's basal metabolic rate B and body mass M are related by

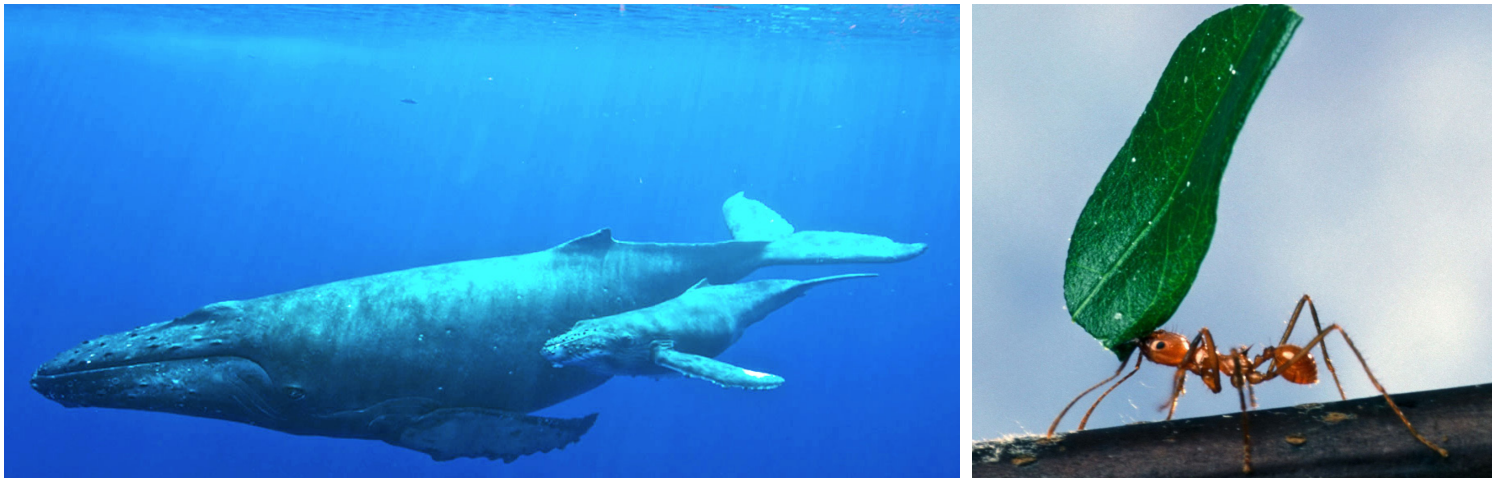

Figure 1. (a) Humpback whales typically have masses of about 30,000 kilograms, and (b) ants have masses of just a few milligrams. Are there fundamental biological principles that are generally valid, even over such an enormous size range?

$$B = B_0 M^{\frac{3}{4}}, \quad (2)$$

where B_0 is a normalization constant. Basal metabolic rate is the rate at which an organism expends energy, while in a resting state, in order to support basic life functions such as tissue maintenance. For ectothermic (cold-blooded) animals, basal metabolic rate is sometimes referred to as standard metabolic rate, or SMR (Auer et al. 2014). Kleiber and Brody's result was counter to the long-held "conventional wisdom", as many biologists were expecting the exponent in Eq. (2) to be ⅔. Their reasoning was that endothermic (warm-blooded) animals must radiate body heat sufficiently quickly to avoid overheating. Since heat is radiated away from a body through its surface, biologists assumed this rate of heat dissipation was proportional to surface area. Surface area is proportional to the square of a linear dimension. And, as mass is proportional to volume, or the cube of the linear dimension, they expected metabolic rate to be proportional to mass raised to the ⅔ power.

Although Kleiber's Law was originally obtained for just mammals and birds, many consider it more widely applicable, to cold-blooded organisms, trees, unicellular organisms, and even molecular processes within the cell. If this is true, Kleiber's Law accounts for a range of masses that varies by 27 orders of magnitude!

Over time, numerous empirical relationships were revealed in addition to Kleiber's Law. But these lacked an overarching theoretical framework to explain the observations. Plant biologist Karl Niklas (2004, p. 872) explains why such a theoretical framework is so important:

> If certain trends are size-dependent and 'invariant' with regard to phyletic affinity or habitat, they draw sharp attention to the existence of properties that are deeply rooted in all, or at least most living things. Identifying these properties using a first principles approach, therefore, has become something of a Holy Grail in biological allometry because any successful theory would unify as many diverse phenomena in biology as Einstein's general theory of relativity has for physics. It is understandable, therefore, that numerous attempts have been made to provide an all-inclusive, unifying theory for broad interspecific trends. However, most have not held up against well-reasoned criticism or withstood empirical tests.

Hence, allometry is of great possible interest to biologists, both creationist and evolutionist.

III. THE WEST, ENQUIST, AND BROWN (WBE) ALLOMETRIC THEORY

A. Overview

Physicist Geoffrey West and biologists Brian Enquist and James Brown (West et al. 1997) have published a theoretical justification for many of the observed allometric scaling laws, including Kleiber's Law. They then explained their metabolic scaling theory (MST) (Tredennick et al. 2013), in greater detail in subsequent papers (Brown et al. 2000; West et al. 2000). They also extended it to include allometric patterns in angiosperm trees (Enquist et al. 2000), as well as the ontogenetic growth of an organism over the course of its lifespan (West et al. 2001). They think the model also has ecological applications, and they provide a heuristic explanation for the fact that tree population density is inversely proportional to individual body mass raised to the ¾ power (Enquist and Niklas 2001; West and Brown 2005). With the exception of a very short book review (Hebert 2022), these developments have gone virtually unnoticed in the creation literature. The following discussion is an overview of the theory, its main assumptions, and its predictions. Detailed derivations of some of the theory's key features are provided in the appendices.

WBE modelled an organism's fluid distribution network as a hierarchical branching network (Fig. 2) of $N + 1$ levels of interconnected cylindrical pipes. For animals, particularly mammals and birds, the highest level of the network, denoted by $k = 0$, is a single pipe, such as the aorta within the human cardiovascular system. Note that this model only includes arteries; it does not attempt to take into account the venous network. This single pipe branches into a number of smaller pipes in the $k = 1$ level and subsequent levels. Let N_k denote the number of pipes within the kth level of the network. Each pipe in the kth level will diverge into two or more pipes which are part of the $k + 1$ level. The number of new pipes at each branching point is the "branching ratio", denoted by n. If we assume the branching ratio n is a constant, say $n = 2$ or $n = 3$, then it follows that the number of pipes in each level of the network is $N_k = n^k$ (Fig. 2). Because the network is assumed to be in steady state, and because an incompressible fluid cannot "pile up" at network junctions, the rate of fluid flow in the single pipe corresponding to $k = 0$ must equal the total fluid flow in each level of the network:

$$\dot{Q}_0 = N_k \dot{Q}_k = n^k \dot{Q}_k \quad (3)$$

Eq. (3) must hold for all values of k in the network, including $k = N$. Within each level, each pipe has a length l_k and radius r_k (Fig. 3). Fluid within each pipe is driven by a pressure gradient Δp_k. This pressure gradient can in principle be provided by a pulsatile pump, as in the case of the mammalian cardiovascular system, or it could be an osmotic vapor pressure gradient, as in the case of a vascular plant.

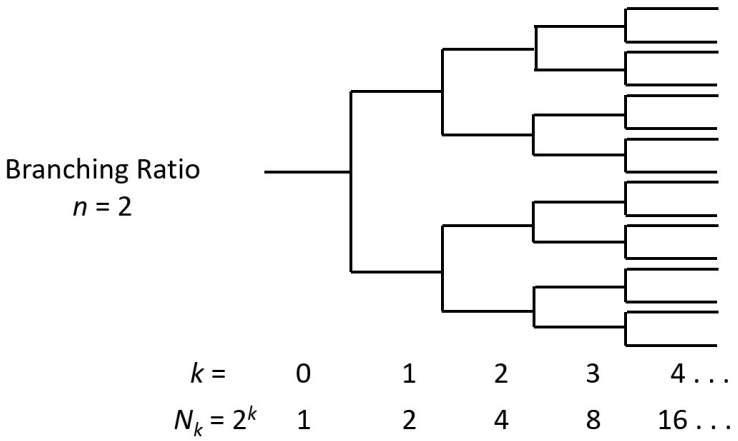

Figure 2. Schematic showing the relationships between levels and branches within the West, Enquist, and Brown (WBE) hierarchical nutrient supply network.

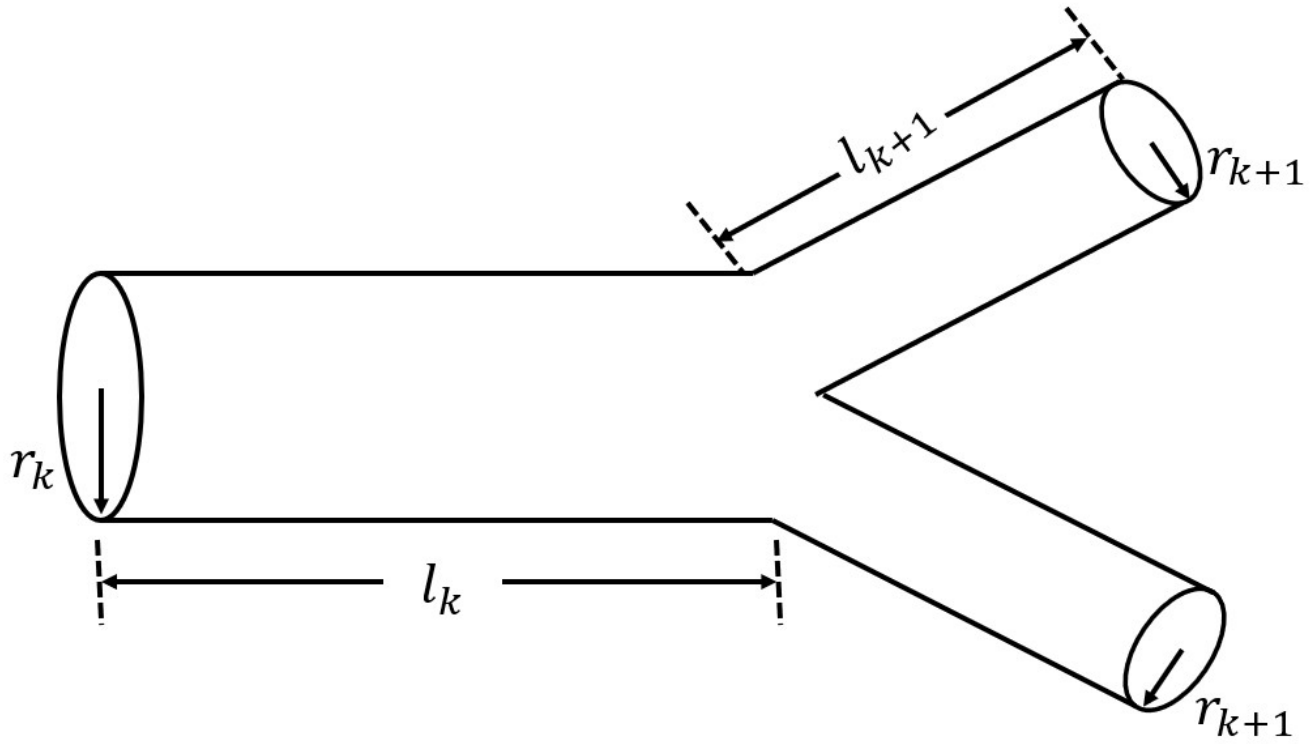

Figure 3. Relationships between vessel radii and lengths in two adjacent levels of the network.

The model has three main assumptions:

Within the $k = N$ level of the network, the pipe sizes are "size invariant." In other words, the length l_N and radius r_N of the very smallest pipes (e.g., capillaries in mammals or birds) do not depend on the mass M of the organism. These characteristic sizes are determined by basic physical principles and limitations, not by the overall size specifics of the organism itself. Capillaries in different creatures should be the same size, regardless of differences in their masses: a capillary in a dinosaur should be the same size as a capillary in a mouse.

Organisms minimize the energy needed to transport materials through the network. This is *prima facie* evidence that organisms were intelligently engineered, although evolutionists attribute this optimization to evolution and natural selection (Brown et al. 2000). However, the WBE model itself makes no evolution-based assumptions. If not for the perfunctory (and apparently obligatory!) assertion that such optimization is achieved by natural selection, the WBE theory could easily be viewed as a design-based theory.

The hierarchical branching network is "volume-filling" in order to ensure that nutrients are supplied to the entire organism's volume. Because this requirement is often poorly explained in the technical literature, I elaborate on it below.

B. Volume-filling

One can imagine that each terminal pipe (capillary) in the network provides nutrients to a group of cells having a "service volume" v_N. Each service volume may be thought of as a biological "black box". We do not necessarily know the precise shape of each service volume. However, because these nutrient-carrying vessels are narrow, we know that the radius of each vessel is much smaller than its length. It is therefore reasonable to assume that $v_N \propto l_N^3$ (Fig. 4). In other words, the service volume is proportional to the length of the capillary which supplies nutrients to it. Because the network must supply nutrients to the organism's entire volume V, the organism's total volume V must equal the sum of the N_N service volumes (Fig. 5a):

$$V = N_N v_N \propto N_N l_N^3 \tag{4}$$

Note that the number of service volumes N_N is also equal to the number of capillaries. However, what is counted as a service volume is somewhat arbitrary. One could, without loss of generality, treat the capillaries themselves as belonging to the service volumes (Fig. 5b). In that case, the service volumes are a little larger. Their volumes are proportional to, not the cube of the pipe lengths in level N, but to the cube of the pipe lengths in level $N-1$. But the number of service volumes has now decreased to N_{N-1}, rather than N_N. However, the organism's entire volume must still be supplied with nutrients:

$$V = N_{N-1} v_{N-1} \propto N_{N-1} l_{N-1}^3 \tag{5}$$

West et al. implicitly assume that the proportionality constant is the same in both cases, although they acknowledged that this "volume-filling" assumption breaks down somewhat for small values of k or N (West et al. 2000). Ignoring this complication, we have for every level (every value of k) within the network:

$$V \propto N_k l_k^3 \propto N_{k+1} l_{k+1}^3 \tag{6}$$

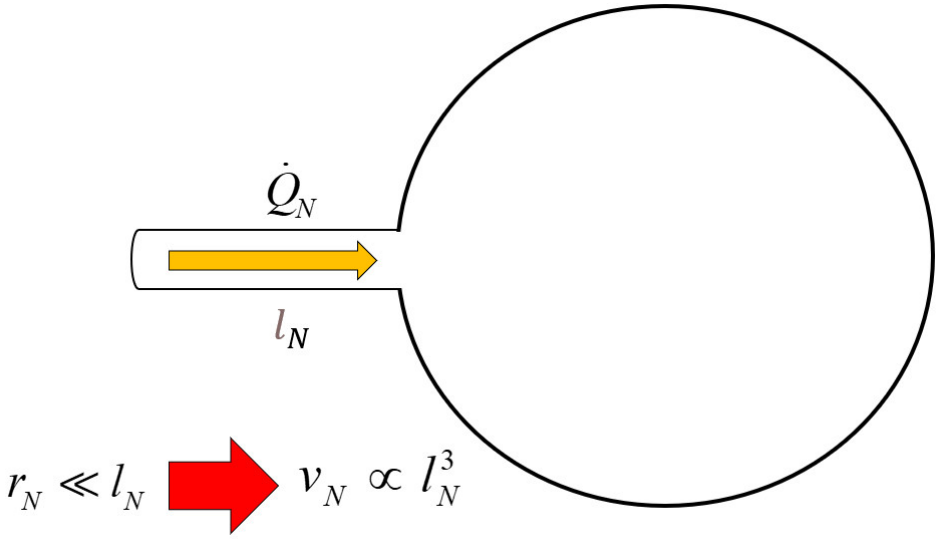

Figure 4. Because the radius of a terminal branch r_N within the network (i.e., a capillary in the mammalian cardiovascular system) is much smaller than its length l_N, it is reasonable to assume that the "service volume" v_N of biological material supplied by each terminal branch is proportional to l_N^3.

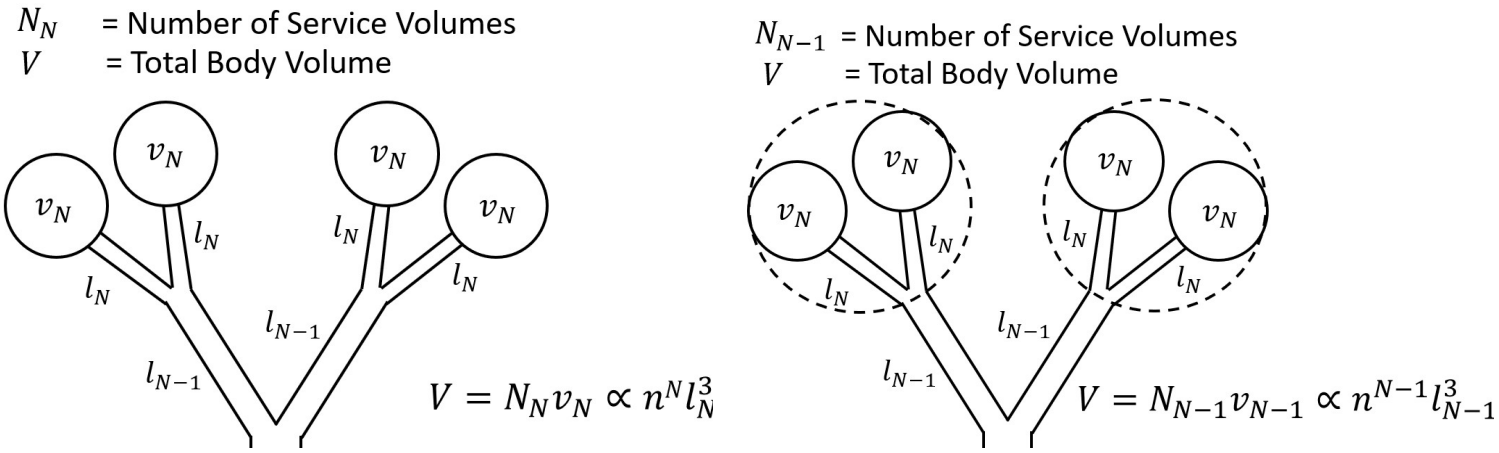

Figure 5. An organism contains N_N service volumes, each with individual volume $v_N \propto l_N^3$. (a) Because an organism's entire volume must be supplied with nutrients, $V = N_N v_N$. (b) But one may treat the terminal branches themselves as being part of each service volume. In that case, there are only N_{N-1} service volumes, each with a volume proportional to l_{N-1}^3. Because the organism's entire volume V must still be supplied we have $V = N_{N-1} v_{N-1}$. In general, $V = N_k v_k \propto N_k l_k^3$, for all k. Note: the radius of v_N and l_N are not to scale.

Inspection of Fig. 2 shows that, in addition to being the number of new pipes at each junction node (or branching point), n is also the ratio of the number of pipes in level $k + 1$ compared to the number of pipes in level k:

$$n = \frac{N_{k+1}}{N_k} \tag{7}$$

Eqs. (6) and (7) gives us the "volume filling" or "space filling" constraint that must be met by the network:

$$\gamma_k = \frac{l_{k+1}}{l_k} = \left(\frac{N_{k+1}}{N_k}\right)^{-\frac{1}{3}} = n^{-\frac{1}{3}} \tag{8}$$

Because the branching ratio n is assumed to be the same for all values of k, γ_k equals γ, a constant.

C. Minimizing power losses in the cardiovascular system

Biologist Cecil D. Murray (1926) suggested that the human cardiovascular system was constructed in such a way as to minimize the work required to oxygenate the body, and he provided simple calculations to demonstrate that construction. J. R. Womersley (1955) published a mathematical solution for velocity, flow rate, and viscous drag in arteries and noted a phase-lag between pressure gradient and flow, similar to the voltage-current phase lag that can exist in an alternating electrical circuit. Womersley did not explicitly state all the details of his derivation, but Shirazi (1972) "fills in" the details. Womersley's solutions strongly suggest that the cardiovascular system is designed to minimize energy losses as oxygenated blood is transported throughout the body.

Within a mammalian or avian cardiovascular system, energy losses

arise from two sources, (1) friction between blood and the vessel wall and (2) impedance losses due to reflection of pulsatile waves at a branch junction. In narrow diameter blood vessels, the blood vessel's high surface area to volume ratio implies that a large fraction of the fluid will be in contact with the vessel walls. Hence, dissipation due to friction is most important in narrow vessels. One may use the method of Lagrange multipliers (Thomas and Finney 1988) to show that power losses in narrow blood vessels are minimized when

$$\beta_k = \beta = \frac{r_{k+1}}{r_k} = n^{-\frac{1}{3}} \tag{9}$$

In this case, total cross-sectional area of the vessels does not remain constant, but increases as k increases. Details of the derivation are provided in Appendix A.

In contrast, the smaller surface area to volume ratio found in wide blood vessels implies that friction is not the most important source of dissipation for wide blood vessels. Rather, dissipation due to reflection at node junctions is the dominant source of power loss. This power loss may be completely eliminated via the process of impedance matching. Doing so (details are in Appendix B) yields the result

$$\beta_k = \beta = \frac{r_{k+1}}{r_k} = n^{-\frac{1}{2}} \tag{10}$$

For wide-diameter blood vessels (lower values of k), cross-sectional area of the network remains constant. This is consistent with observations that the cross-sectional area of the vascular bed stays constant in both humans and dogs until the vessels reach a transitional size, at which point the area of the bed begins to increase (Caro et al. 2012, p. 244).

In the supplementary material to their paper, Savage et al. (2008) provide the outline for the more general case of rigid blood vessels of any radius. Although this derivation neglects blood vessel elasticity, it still gives the exact result for narrow elastic blood vessels and results that are very close to the exact answer for wide elastic blood vessels. Hence, their simplified derivation illustrates the important features of the *much* more complicated exact solution (Womersley 1955, Shirazi 1972) for elastic blood vessels. The general solution provides radius scaling given by Eq. (9) for very narrow blood vessels, and radius scaling given by Eq. (10) for very wide blood vessels.

This optimization of the circulatory system is so obvious that scientists cannot help but use words like "design" when describing the circulatory system. Li (2000, p. 113) states, "The optimal design features of the mammalian cardiovascular system have been marveled at by us *Homo sapiens* for many decades." Li goes on to say (2000, pp. 125-126)

> Invariant pulse transmission features are embedded in the similar pulse pressure and flow waveforms observed at corresponding anatomical sites. The precision of natural design is even more amazing at vascular branching junctions, where branching vessel impedances are practically matched to ensure pulse wave transmission at utmost efficiency with minimal wave reflection and energy losses.

That similar cardiovascular transmission features are observed at "corresponding anatomical sites" for different animals seems too unlikely a coincidence to attribute to "convergent evolution". In the introduction to his detailed derivation of Womersley's (1955) results, Shirazi (1972, p. 2) states

> Womersley's work forms an important link in the continuing chain of understanding [of the cardiovascular system]. We have chosen to present his version not because it is the most sophisticated work in this area but because within its limitations it is a well-developed treatment of several aspects of the arterial problem, and *suggests a rational basis for many of the peculiar characteristics observed in the mammalian cardiovascular system*. [emphasis mine]

Yet Brown et al. (2000, p. 11) instead attribute such features to natural selection: "Natural selection for efficient design of such distribution and support . . . has resulted in the evolution of networks with self-similar, hierarchically scaled architectures." Yet, isn't it reasonable to ask if the phrase "natural selection for" doesn't "smuggle in" the same intelligent intentionality to presumed naturalistic explanations that is attributed to an intelligent Designer by other scientists? After all, "selection" is always rooted in intelligence and volition, while the word "for" in this context indicates purposeful intentions with the definitive target of "efficient design." If evolutionary biologists who proceed from an interpretive framework of naturalism have not really provided a non-intelligent explanation, but instead injected a substitute intelligence cloaked in selectionist jargon, then isn't creation by an intelligent Engineer a more plausible explanation? After all, design by an intelligent Engineer explains 1) optimized features, that 2) can be reduced to mathematical formulas, and 3) operate by the same engineering principles as human-engineered fluid-transport systems.

D. Deriving Kleiber's Law

The results of the previous two sections suggest that the way to minimize energy losses due to *both* friction and reflection is to apply the volume-filling constraint of Eq. (8) for all values of k, the constraint of Eq. (9) for narrow blood vessels (higher k values) and the constraint of Eq. (10) for wide blood vessels (smaller values). This may be done with a "transitional" value of $k = \bar{k}$, as illustrated in Fig. 6.

Savage et al. (2008) explain more clearly the derivation of Kleiber's Law, some details of which are omitted in West et al. (2000). A key step in this derivation is the realization that blood volume V_b is proportional to the organism's mass M. We follow their derivation in Appendix C. They obtain

$$M = A_0 B^{\frac{4}{3}} \left(1 + A_1 B^{-\frac{1}{3}}\right) \tag{11}$$

Here A_0 and A_1 are mass-independent constants. Strictly speaking, the relationship above between body mass M and basal metabolic rate B only becomes Kleiber's Law in the limit of infinite mass (Savage et al. 2008). Hence, deviations from Kleiber's Law are more likely for smaller organisms, and this may help to explain some of the contrary results mentioned in Section IV.

WBE demonstrated quite a few allometric relationships for char-

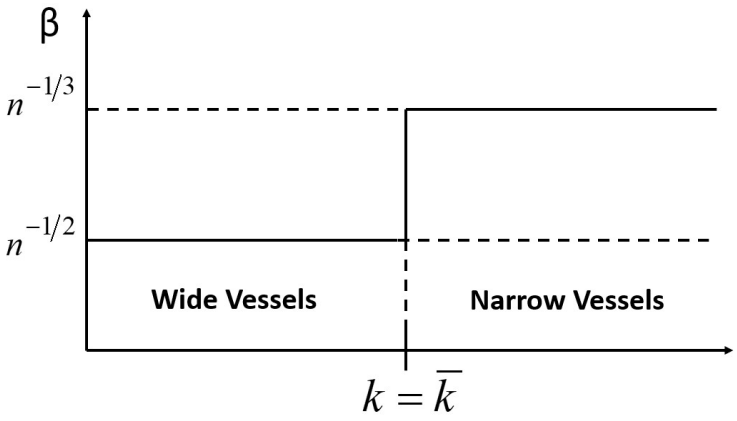

Figure 6. Higher cardiovascular efficiency is obtained by using the "area-preserving" $n^{-½}$ radius- scaling for wide blood vessels (smaller values of k), and the $n^{-⅓}$ radius-scaling for thin blood vessels (higher values of k). After Figure 8 in West, Brown, and Enquist (2000).

acteristics of the cardiovascular and respiratory systems, some of which have already been confirmed experimentally (Tables 1 and 2).

E. Angiosperm trees

An extension of their theory for broad-leaved angiosperm trees also makes some successful predictions, perhaps most notably that maximum possible tree heights should be on the order of 100 meters. This is in agreement with observations: the world's tallest tree is a coastal redwood (*Sequoia sempervirens*) named "Hyperion" with a height of 116 meters (Enking 2022). For purposes of brevity, we do not discuss it here. However, interested readers may consult Enquist et al. (2000) for details.

F. WBE ontogenetic growth theory

West et al. (2001) also developed a general model for the ontogenetic growth of an organism, i.e., growth over the course of its lifetime. Their model partitions metabolic energy use between the energy needed to maintain existing tissue and the energy needed to produce new tissue:

$$B = \sum_c \left[N_c B_c + E_c \frac{dN_c}{dt} \right] \tag{12}$$

The total basal metabolic rate B is the sum of the individual metabolic rates of the body's cells, plus the rate at which energy is used to form new cells. The summation is over the different tissue types within the body. For each tissue type, there are N_c cells, each having a cellular metabolic rate of B_c, and E_c is the energy needed to form a new cell for that particular tissue type. WBE used Eq. (12) to derive an expression (see Appendix D for details) for an organism's body mass m as a function of time:

$$\left(\frac{m}{M}\right)^{1/4} = 1 - \left[1 - \left(\frac{m_0}{M}\right)^{1/4}\right] e^{\frac{-aM^{-1/4}}{4}t} \tag{13}$$

Table 1. WBE predicted values of λ in cardiovascular allometric relationships $Y = Y_0 M^{\lambda}$, as well as experimentally-determined values (with references).

Variable	Symbol	Predicted Exp.	Empirical Exp.	Reference
Aorta Radius	r_0	$3/8 = 0.375$	0.36, 0.41	Holt et al., Schmidt-Nielsen
Pressure in Aorta	Δp_0	$0 = 0.00$	0.032	
Blood Velocity in Aorta	u_0	$0 = 0.00$	0.07	
Blood Volume	V_b	$1 = 1.00$	0.99, 1.00, 1.02	Günther, Prothero, Stahl
Circulation Time	T	$1/4 = 0.25$	0.25	Schmidt-Nielsen (calculated)
Circulation Distance	l	$1/4 = 0.25$	ND	
Cardiac Stroke Volume		$1 = 1.00$	1.04-1.05	Günther
Cardiac Frequency	ω	$-1/4 = -0.25$	−0.25, −0.26	Stahl, Günther
Cardiac Output	E	$3/4 = 0.75$	0.81, 0.78–0.79	Stahl, Günther
Number of Capillaries	N_c	$3/4 = 0.75$	ND	
Supply Radius of Cells		$1/12 = 0.083$	ND	
Radius of Krogh Cylinder		$1/8 = 0.125$	ND	
Density of Capillaries		$-1/12 = -0.083$	−0.095	
Oxygen Affinity of Blood	P_{50}	$-1/12 = -0.083$	−0.089	
Total Peripheral Resistance	Z	$-3/4 = -0.75$	−0.76	Günther
Womersley Number	α	$1/4 = 0.25$	0.25	
Metabolic Rate (O_2 Uptake)	B	$3/4 = 0.75$	0.76	Stahl

Table 2. WBE predicted values of λ in respiratory allometric relationships $Y = Y_0 M^{\lambda}$, as well as experimentally-determined values (with references).

Variable	Symbol	Predicted Exp.	Empirical Exp.	Reference
Lung Volume		$1 = 1.00$	1.05	Weibel
Respiratory Frequency		$-1/4 = -0.25$	$-0.26, -0.28$	Stahl, Tenney & Bartlett
Volume Flow to Lung		$3/4 = 0.75$	0.80	Stahl
Interpleural Pressure		$0 = 0.00$	0.004	Günther
Trachea Diameter		$3/8 = 0.0.375$	0.39	Tenney & Bartlett
Air Velocity in Trachea		$0 = 0.00$	0.02–0.04	Calder
Tidal Volume		$1 = 1.00$	1.04	Stahl
Power Dissipated		$3/4 = 0.75$	0.78	Stahl
Number of Alveoli	N_A	$3/4 = 0.75$	ND	
Volume of Alveolus	V_A	$1/4 = 0.25$	ND	
Radius of Alveolus	r_A	$1/12 = 0.083$		
Surface Area of Alveolus	A_A	$1/6 = 0.083$	0.095	Gehr et al.
Surface Area of Lung	A_L	$11/12 = 0.92$		
Oxygen Diffusing Capacity		$1 = 1.00$	0.96, 0.99, 1.18	Weibel, Gehr et al., Stahl
Total Airway Resistance		$-3/4 = -0.75$	-0.70	Stahl
O_2 Consumption Rate		$3/4 = 0.75$	0.76, 0.72	Stahl, Weibel

Here M is the organism's final mass at maturity, m_0 is the organism's mass at birth, and a is a taxon-specific constant.

Their model results in a sigmoid "universal growth curve" (Fig. 7) for fraction of adult body mass as a function of time since birth. It does a good job of predicting the shape of growth curves for guinea pigs, guppies, hens, and cattle, as well as general sizes for nine other examples of fish, mammals and birds (West et al. 2001). This model, or one similar to it, might eventually help creationists explain the extreme longevity of pre-Flood humans, as discussed in Section VC.

IV. WBE THEORY: CRITICISMS AND ALTERNATIVES

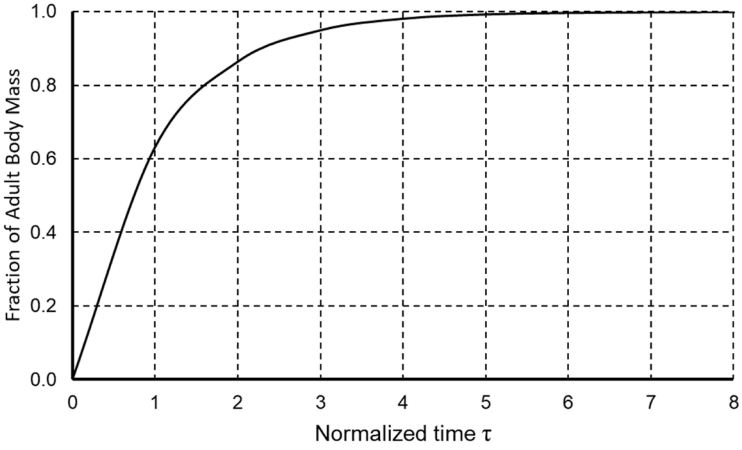

Figure 7. The sigmoid growth curve derived by WBE, showing fraction of adult body mass as a function of (normalized) time τ since birth.

The WBE theory is not without criticism. Glazier (2006) argues that Kleiber's Law, which the WBE theory explains, is not truly universal. Dodds et al. (2001) and White and Seymour (2003, 2005) argue that statistical evidence is consistent with $\lambda = ⅔$, rather than ¾. WBE have defended their research against these criticisms (Brown et al. 2005; West and Brown 2005). West and Brown (2005) point out that Calder (1984), McMahon and Bonner (1983), Schmidt-Nielsen (1986), and Peters (1993) all independently concluded that quarter-power scaling in biological systems was both real and ubiquitous.

Kozłowski and Konarzewski (2004, 2005) and Etienne et al. (2006) have criticized the underlying logic of the WBE model. Hulbert (2014) argues that Kleiber's law is an "empirical approximation", not a rule or law. Price et al. (2011), Bentley et al. (2013), Tredennick et al. (2013) and Price et al. (2022), have noted observations that contradict or potentially contradict the theory, as has Niklas (1995, 1997). Nevertheless, Niklas thinks WBE are "on the right track", so to speak, and he goes so far as to say that, although much work remains to be done, a unifying allometric theory regarding plant biology is "near at hand" (2004, p. 871).

Nor is the WBE theory the only metabolic scaling theory. For instance, Price et al. (2022), have produced an alternate theory for land plants, one that utilizes velocity constraints and conservation of volume flow rate throughout the organism. Escala (2019) used dimensional analysis (McMahon and Bonner 1983) to obtain an analogue to Kleiber's Law in which the rate of oxygen consumption is proportional to the product of body mass, some characteristic body frequency (such as respiration or heart rate), and the mass of oxygen utilized per unit of body mass. Unlike the WBE theory, his result

does not depend upon the units used to measure basal metabolic rate or mass, as should indeed be the case for a true physical law. In Escala (2022) he improved upon his result by including temperature as a variable. Escala's work may be of particular interest to creationists for reasons explained in Section VB.

V. AVENUES FOR FUTURE CREATIONIST RESEARCH

Metabolic scaling theories suggest real possibilities for future creation research. Obviously, creationist biologists and biophysicists could work on improving such theories by incorporating still more design constraints in biological models. However, this may make the mathematics of such models intractable, at least for the foreseeable future. Ontogenetic scaling theories, however, offer much more practical opportunities.

A. Ontogenetic growth theory and giantism

Allometric scaling may be helpful in explaining the phenomenon of giantism, which has long been of interest to creationists. Giantism is likely caused by multiple factors. Biologists have long noted the "island rule" that small vertebrates living on islands are often larger than their mainland counterparts, while larger vertebrates shrink in size when they colonize islands (Lomolino 2005). This insular giantism/dwarfism is often accompanied by longer life spans and smaller reproductive outputs (Baxter-Gilbert et al. 2020).

Reduced reproductive output in island populations makes sense as an innate design feature, as this could be a means that the Lord uses to prevent overpopulation in island settings. If so, insular giantism and dwarfism might be adaptive design features, as well. It is worth noting in passing that evolutionists worried about "overpopulation" seem to fail to consider the possibility that living things might self-adjust reproductive rates to adjust to higher or lower population densities. The ability of organisms to modulate their sizes and reproductive rates in response to changing environmental conditions could be another example of the ability of organisms to self-adjust as they continuously track their environments (Guliuzza and Gaskill 2018).

Likewise, Ice Age megafauna (birds and mammals) may have grown larger to minimize heat losses in cold environments, per "Bergmann's rule" (Bergmann 1847). It is also possible that at least some animals were still experiencing relatively long lifespans in the immediate post-Flood world. Hence, longer lifespans might have contributed to larger sizes for some of these animals.

As discussed above, West et al. (2001) have developed a general model for the growth of an organism over the course of its lifetime, and it, combined with biblical considerations, may be helpful in explaining the large sizes of many animals in the pre-Flood world.

Before continuing this discussion, we define the terms *determinate growth* and *indeterminate growth*. Organisms with determinate growth stop growing at maturity, whereas organisms with indeterminate growth do not. Of course, growth is really only *apparently* indeterminate, as there are physical limits to how big an organism can become. For example, J. B. S. Haldane (1927) used Galileo's area-volume law to observe that a giant ten times the height of a normal man would be physiologically impossible, since increasing a man's height by a factor of ten would make him a thousand times heavier, but the strength of his bones and muscles, being proportional to their cross-sectional area, would only become one hundred times stronger. Since a stress ten times greater than that due to body weight is sufficient to fracture a bone, such a giant would be in danger of breaking his leg simply by taking a step! Of course, this problem does not necessarily apply to the giants described in Scripture, with their much more realistic and physically plausible heights (e.g., I Samuel 17:4). It is also possible that these biblical giants were not precisely "scaled up" versions of normal-sized humans. At these larger sizes, allometric factors may have come into play, such as the development of somewhat thicker bones.

In any case, it would seem that within a creationist paradigm, *all* growth is determinate growth, as God in His wisdom would put limits on the maximum sizes that could be attained by living creatures. This is especially clear when we consider that there was no death in the pre-Fall world. Organisms not subject to death simply could not keep growing without limit, as their sizes would eventually become physically untenable. Hence, God must have placed pre-determined limits on the sizes of living things. So what we observe as *apparently* indeterminate growth might simply be the result of much shorter lifespans than those attained to in the pre-Flood and immediate post-Flood worlds. Creationists have long noted the large sizes of many now-extinct animals (Nelson 2017) and have suggested (Beasley 1990) that longer lifespans allowed pre-Flood creatures to attain larger sizes at maturity than in today's world. It may be that creatures today with (apparently) indeterminate growth simply don't live long enough to attain their maximum possible physical sizes. For instance, sharks and reptiles are generally indeterminate growers (Hariharan et al. 2016). It is not hard to imagine that the megalodon may have been a fully mature great white shark of extreme age, and we discuss evidence for this possibility in Section VC.

In an online pre-print of a paper that has admittedly not yet been peer-reviewed, Escala (2021) makes predictions about the time for an organism to reach maturity compared to its maximum possible lifespan. Hence it may be of interest to creationists attempting to explain the great longevity of pre-Flood humans. For simplicity, his predictions, unlike Escala (2022), do not take into account possible variations in temperature or oxygen consumption, but it might be possible to take those variations into account in future studies. Both evolutionists and creationists have long-speculated that higher atmospheric oxygen concentrations may have contributed to past giantism of some organisms (Dillow 1982; Harrison et. al. 2010, Wieland and Sarfati 2011). Likewise, creationists (Whitcomb and Morris 1991, Dillow 1982) have long suspected that average global temperatures in the pre-Fall world were higher than today, even if the cause of a warmer climate is unknown. Hence, a more sophisticated version of Escala's work might enable creation researchers to at least partially explain why post-Flood lifespans are so much shorter than pre-Flood lifespans.

B. Longevity: linking theory to observations

In Genesis 5, the youngest age listed at which a patriarch's son is born is 65 (Genesis 5:15, 21). Although some, perhaps many, of these sons were probably not first-born, it seems unlikely that *none*

of them were. And, given the strength of the human sex drive, it also seems very unlikely that all these patriarchs were choosing to postpone marriage thirty or forty years after reaching sexual maturity! This seems to strongly suggest slower growth and development, as suggested by Cuozzo (1998b). If the pre-Flood patriarchs did not reach sexual maturity until roughly 65 years of age, this fits with empirical evidence that age at sexual and/or skeletal maturity positively correlates with lifespan, i.e., the longer an organism takes to reach maturity, the longer its lifespan. Studies have demonstrated this to be true in general for terrestrial vertebrates, including birds and reptiles (de Magalhães et al. 2007, Ricklefs 2010a), as well as particularly true for bivalve molluscs (Abele et al. 2008, Ridgeway et al. 2011, Moss et al. 2016), fish (Genade et al. 2005, Lee, Monaghan, and Metcalfe 2013), and birds and mammals (Ricklefs 2010b). A good overview is provided by Marchionni et al. (2020).

There is also evidence (de Magalhães et al. 2007, Ricklefs 2010a, Ridgway et al. 2011) that larger body size at maturity is positively correlated with greater longevity, although there is conflicting evidence in the case of bivalve molluscs: Ridgway et al. (2011) found a weak but statistically significant correlation, but a larger study by Moss et al. (2016) did not. For the time being we do not attempt to explain these general observations, rather we simply accept them as empirical facts. In general, greater longevity seems to be positively correlated with greater ages and sizes at maturity. Because the WBE ontogenetic growth model makes predictions about the time for an organism to attain its maximum size (Appendix D), it or a similar theory could shed light on this issue and yield insights into pre-Flood and immediate post-Flood environmental conditions. With this in mind, I discuss below five possible lines of evidence for extreme animal longevity in the pre-Flood and immediate post-Flood worlds.

C. Possible paleo-ontogenetic evidence for extreme animal longevity

The WBE ontogenetic theory provides a theoretical justification for why animal age-versus-mass growth curves exhibit an almost-universal 'sigmoid' shape (Fig. 7). Biologists have long-used the similar-looking empirical Bertalanffy growth curve (1938) to describe the linear growth of an organism:

$$L(t) = L_{\infty}\left(1 - e^{-k(t-t_0)}\right) \tag{14}$$

Here, $L(t)$ is the length of a major body dimension of the animal, say height or length. L_{∞} is the animal's body length at maturity. The parameter k is a measure of how quickly the animal grows, and t_0 is the (theoretical) age at which the animal has a size of zero. Eq. (14) indicates a period of rapid juvenile growth followed by a slowing or stopping of growth at adulthood. Although the mathematical form of Eq. (14) is not identical to that of Eq. (13), this period of rapid linear growth clearly corresponds to the steeply-sloped portion of Figure 7, whereas the period of very slow growth corresponds to Figure 7's plateau.

The WBE ontogenetic theory does not tell us anything about how long an animal will live *per se*. It simply describes how the mass of the animal varies as a function of time. However, we have already noted that there is considerable empirical evidence that both higher age and larger body size at maturity are positively correlated with greater longevity in extant animals. This is a particularly intriguing observation in light of the large body sizes of many pre-Flood creatures. We now briefly discuss five possible lines of fossil evidence (already published in the mainstream evolutionary literature) that animals, as well as humans, were experiencing much greater longevity than do comparable extant animal forms.

However, before doing so, we need to address possible objections to such comparisons. In order to determine whether or not living animal representatives are shorter-lived than their pre-Flood ancestors, we need to compare ontological data from both before and after the Flood. In many cases, it is not possible to perform a true species-to-species comparison, as many fossil species are now extinct. However, the examples below involve comparisons between creatures with similar body structures, even if they have been grouped in different species or genera. Moreover, it is possible to use a calculated "index of growth performance" (Pauly and Munro 1984) to compare growth rates between different species, provided the species have similar body shapes (Killam et al. 2021). Also, given the "over-splitting" tendencies of many taxonomists, it is quite likely in many cases that different but similar species actually belong to the same Genesis kind. Hence, we should not let this prevent us from making reasonable comparisons, even if they are not necessarily intraspecific.

Such a comparison implicitly assumes that paleontologists are accurately identifying and counting growth bands in shells, bones, and osteoderms. Or at the very least, it assumes that any systematic error in counting growth bands in pre-Flood fossils will be the same as any systematic error in counting growth bands in post-Flood remains. Note that the bands do not even necessarily need to be annual. As long as growth bands formed in the pre-Flood world represent the same units of time (years, months, or days) as in the post-Flood world, it is possible to compare pre- and post-Flood lifespans, even if we are unsure of the precise units of time that each band represents. I think we can be reasonably confident in these reconstructions, but I recognize the need for creationists to study their underlying assumptions more deeply before making strong claims in this regard.

1. Larger animal sizes

Many creationists (e.g., Beasley 1990) have long-suspected that the giant sizes of many extinct fossil forms were linked to greater past longevity. Earlier in this section I cited, for extant animals, positive correlations between greater body size at maturity and greater longevity. If such a correlation held for extinct forms as well, then the large sizes of these fossil forms may be indirect evidence that they were long-lived. The particular case of sauropod dinosaurs is discussed in Section VD.

2. Long-lived and slow-growing bivalve molluscs

Sclerochronology is the counting of growth bands in hard remans to infer details about an organism's growth and ontogeny (Moss et al. 2021). A number of studies suggest that molluscs in the pre-Flood and immediate post-Flood worlds were experiencing much greater longevity than their modern-day counterparts. Kirby (2001) constructed growth curves for Miocene, Pleistocene, and Recent

Crassostrea oysters. The Miocene shells were obtained from two different locations in California, the Pleistocene shells from Virginia, and the Recent shells from North Carolina. All shells were collected from a relatively narrow latitude band between 34.6° and 36.8° north latitude. The Miocene oysters apparently had much greater maximum lifespans and sizes than the Late Pleistocene and Recent *Crassostrea* oysters (Figs. 8 and 9). In agreement with Holt (1996), Baumgardner (Oard 2002), Oard (2013), and Clarey (2019), I am assuming that, generally speaking, Miocene and Pleistocene strata are Flood and post-Flood strata, respectively. The dramatic decrease in maximum oyster lifespan shown in Figure 8 parallels the dramatic decrease in human lifespan after the Flood described in Genesis 11.

Similar late Cenozoic trends appear in giant clams from the Red Sea region (Killam et al. 2021), *Mercenaria* clams from North Carolina and Florida (Palmer et al. 2021), and venerid bivalves from the Japanese Islands (Sato 1999). These examples are not as dramatic as those shown in Figures 8 and 9 are are perhaps more easily dismissed. Moreover, the pattern is equivocal for chionine bivalves from the tropical Americas (Roopnarine 1996). These examples are not as dramatic as those shown in Figures 8 and 9 and are perhaps more easily dismissed. Moreover, the pattern does not hold for *Mercenaria* clams from Florida (Palmer et al. 2021).

However, strong evidence for greater mollusc longevity in the pre-Flood world comes from Seymour Island, Antarctica. A study of 12 Eocene *Cucullaea raea* shallow-marine clam shells showed "extreme" longevity (Buick and Ivany 2004). Despite the small sample size and the fact that the sample shells were *not* exceptional in size or number of visible bands, all twelve clams were estimated to be at least 50 years old at time of death, with 6 clams more than 90 years old, and 5 clams greater than 100 years old! Buick and Ivany (2004, p. 922) noted, "These are some of the longest-lived clams ever documented from the modern or ancient world."

A larger study showed that 11 species of Cretaceous and Paleogene Seymour Island bivalves were slow-growing and long-lived (Moss et al. 2017, p. 373):

> While a number of modern taxa can attain life spans in excess of 50 years, the modal value of maximum reported life span for bivalve species today is 3 years (Moss et al. 2016). The shortest-lived species measured from Seymour Island reached life spans of at least 22 years. The longevity of bivalves in this assemblage, even as established from such a restricted sample, is impressive.

Moss et al. (2017) noted that different taxonomic groups were well-represented in their study, as they studied fossil assemblages belonging to three different families in three different orders. Moreover, they noted they were likely *underestimating* the ages of these bivalve species due to ring counting difficulties and the relatively small sample sizes of their specimens. Even so, they concluded (Moss et al. 2017, p. 365) that "all 11 species examined are both slow growing and long-lived, especially when compared with modern bivalves in similar temperature settings."

Temperature is indeed an important factor in these kinds of studies. Although extant high latitude marine bivalves can live hundreds of years (Abele et al. 2008), this seems to be a temperature-dependent phenomenon, possibly due to a dramatic slowdown in metabolism triggered by extremely cold temperatures. The longevities of these Seymour Island bivalves are particularly impressive because uniformitarians believe the Antarctic Peninsula experienced relatively warm temperatures during the Cretaceous and Paleogene. And most creationists would probably agree that global temperatures in the pre-Flood world were higher than today's averages. Hence, neither we nor they can use cold temperatures as an explanation for why these particular molluscs lived so long. If anything, such warm temperatures should have sped up their metabolisms, decreasing their longevity. Yet this was not the case.

3. Slowly-maturing birds

Apparently, there is osteo-histological evidence that birds once took longer to mature than they do today. A detailed discussion of osteo-histology is beyond the scope of this paper, but we note in pass-

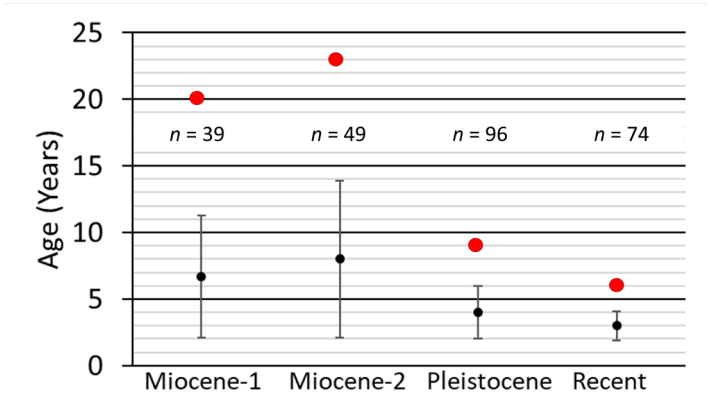

Figure 8. Maximum lifespan (red dots) for four assemblages of California, Virginia, and North Carolina *Crassostrea* oysters all collected between 34.6° and 36.8° north latitude. The maximum lifespans for the Late Pleistocene and Recent oysters are dramatically less than the maximum life-spans for the Miocene oysters. Black dots represent the average age of each assemblage, and error bars are the standard deviations. The number of fossil specimens in each assemblage is shown.

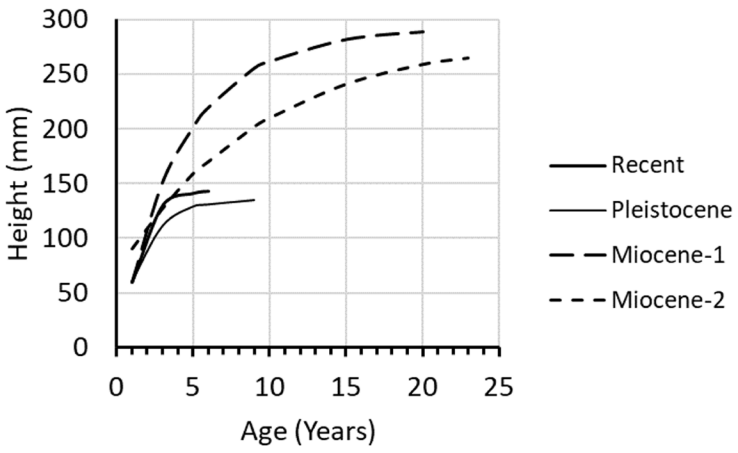

Figure 9. Height-versus-age growth curves constructed for the four *Crassostrea* oyster assemblages whose data are summarized in Figure 8. After Figure 3B in Kirby (2001).

ing some observations from evolutionary paleontologists. Chiappe and Bell (2001, p. 556) state:

> Surprisingly, these [histological] data point at significant differences with respect to living birds. Modern birds usually hatch and develop full-grown sizes within a year. Yet, studies of early birds spread across the evolutionary tree (*Archaeopteryx*, *Confuciusornis*, Enantiornithes and others) reveal that these animals had a protracted period of skeletal growth, in which growth was punctuated by annual pauses (phases when skeletal growth slowed down significantly or virtually stopped).

Padian (2023, p. 252) concurs:

> Birds seem to have inherited both high metabolic rates and high growth rates from their dinosaurian ancestors, but by the time the living groups of birds appeared, they had evolved the even-higher rates of growth and metabolism that are observed today[10]. *The first birds took several years of development to reach skeletal maturity[11], but today's birds can do so within a year or less.*[emphases mine, footnotes in original]

Erickson et al. (2009) note that the "first" birds took longer to mature than most comparably-sized extant birds and that *Archaeopteryx* took longer to mature compared to extant precocial and alticial land birds.

If pre-Flood birds took longer to mature than extant birds, this could be evidence they were living longer than birds of today. However, this pattern may not have held for all ancient birds. According to Feduccia (2006), the bone histology of Cretaceous ornithurines ('ancient' birds similar to 'modern' birds) is similar to that of modern birds, without growth rings. This could suggest shorter growth intervals, lacking in such pauses. However, Foth et al. (2021) note that juvenile avian fossils are rare, and that most paleo-ontogenetic information from birds comes from Enantiornithes, which took longer to reach skeletal maturity than extant birds. O'Connor et al. (2014) note that "growth in Early Cretaceous birds remains poorly understood."

4. Slow-growing crocodylians

Erickson and Brochu (1999) counted growth rings in the dorsal osteoderms of multiple species of fossil crocodylians and used these data to construct estimated age-versus-length growth curves (Figure 10). The growth curves for the two unidentified species of *Deinosuchus* from Texas and Montana suggest that these representatives of the 'terror crocodile' were particularly slow-growing. If the von Bertalanffy age-versus-length curve from Eq. (14) is a universal one, then it seems *Deinosuchus* would have still been an adolescent at 40 or 50 years of age. Moreover, because the two *Deinosuchus* growth curves have not yet 'plateaued' or 'leveled-off', it seems that the maximum sizes of these two particular species (or perhaps single species) of *Deinosuchus* could easily have exceeded nine meters. But whatever their final size, their adult forms clearly would have been much larger than adult sizes of extant crocodylians (Figure 10). Likewise, they took much more time to reach maturity than extant forms. Both observations are suggestive of great longevity.

The other six crocodylian species apparently did not attain ages or sizes as great as those of *Deinosuchus*. Smaller adult size could be an adaptation to different environments in the pre-Flood world. However, it could also be an illusion caused by sampling bias: Could these growth curves have been constructed from fossil assemblages of juvenile crocodylians that were separated from larger adults during the Flood? The *Leidyosuchus*, *Pristichampsus*, and *Brachychampsa* growth curves "track" fairly well (Figure 10) with that of the extant American alligator (*Alligator mississippiensis*), at least for ages less than 25 years. Thus, these particular crocodylians may or may not have taken longer to mature. However, the relatively steep slopes of the "*Crocodylus*" *affinis* and *Borealosuchus* growth curves might imply that these creatures were still 'adolescents' at 20-25 years of age.

The giant *Sarcosuchus imperator* also apparently grew quite slowly. Although I have yet to find growth curve data for this species, Sereno et al. (2001) concluded that *S. imperator* took 50 or 60 years to reach its maximum adult size. Interestingly, Sereno et al. stated in their ab-stract that it had a life-span of 50-60 years. However, this statement is not necessarily correct. Yes, *S. imperator* apparently took 50 or 60 years to reach maturity, but it is obvious that time to maturity is *not* necessarily equal to life-span. The osteoderm data give us clues about *S. imperator*'s time of growth, but they do not tell us anything about how long it *lived*, as least not directly. But its long maturation period and large adult size (estimated weight of 8 metric tons and length of 11 to 12 meters) could both be indicators of greater longevity compared to extant crocodylian forms.

5. "Old" adolescent sharks

Two fossil shark vertebrae suggest that pre-Flood sharks took much longer to grow than extant sharks. By counting presumed annual growth rings in the fossilized vertebrae of a *Ptychodus* shark from Cretaceous strata in Spain, Jambura and Kriwet (2020) inferred that this *Ptychodus* shark was 30 years old at time of death. The inferred growth curve indicated that this shark had not yet reached maturity despite its "old" age. Jambura was quoted as saying (Anonymous, 2020):

> We calculated a size of 4-7 meters and an age of 30 years for the examined shark. It's astonishing that this shark was not yet mature when it died despite its rather old age . . . . [T]his shark doesn't show any signs of flattenings or inflections in the growth profile, meaning that it was not mature – a teenager, if you want. This suggests that these sharks grew even larger and older.

It's even more amazing when one realizes that data from a more complete *Ptychodus* shark fossil (Shimada et al. 2010) suggests that full-grown adults could be 10 to 11 meters long!

Shimada et al. (2021) counted growth rings in a Miocene megalodon vertebrae from Belgium. Their constructed von Bertalanffy growth curve (Figure 11) implies that *Otodus megalodon* would take 498 years to reach 95% of its full adult body length of almost 32 meters. Admittedly, these time and length estimates are probably too high (see downward-pointing arrow in Figure 11), as they imply anterior teeth crown heights more than twice the height of any such megalodon fossil tooth yet discovered. But even if one completely ignores this extrapolation, this particular megalodon was already larger than an extant great white shark at 46 years of age, yet it was apparently

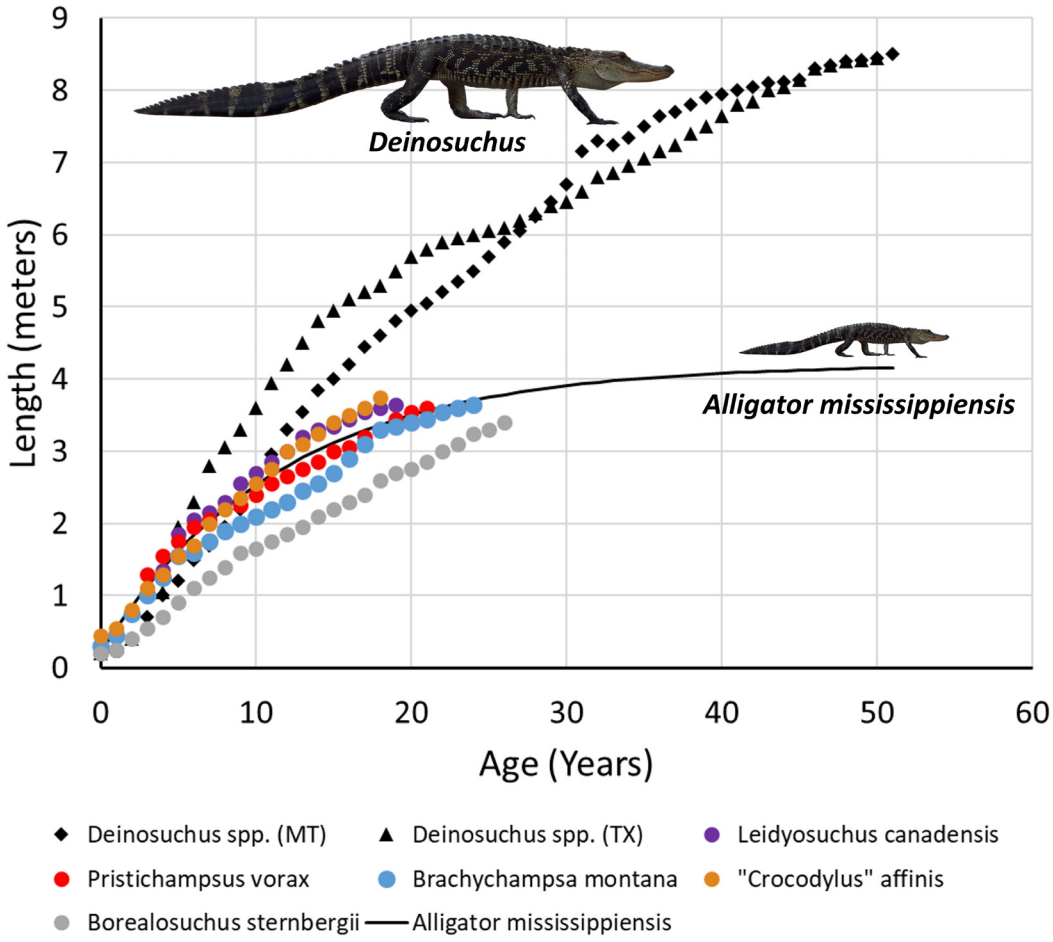

Figure 10. Length-versus-age growth curves constructed for multiple species of fossil crocodylians, after Figure 2a in Erickson and Brochu (1999), including two representatives from the genus *Deinosuchus*. For comparison, the growth curve of the American alligator (*Alligator mississippiensis*) is shown. American alligator growth curve obtained from a catch-tag-and-release study (Chabreck and Joanen, 1979) of thousands of individuals from Louisiana, USA. Alligator image credit: Gareth Rasberry, CC BYSA 3.0 <https://creativecommons.org/licenses/by-sa/3.0>, via Wikimedia Commons.

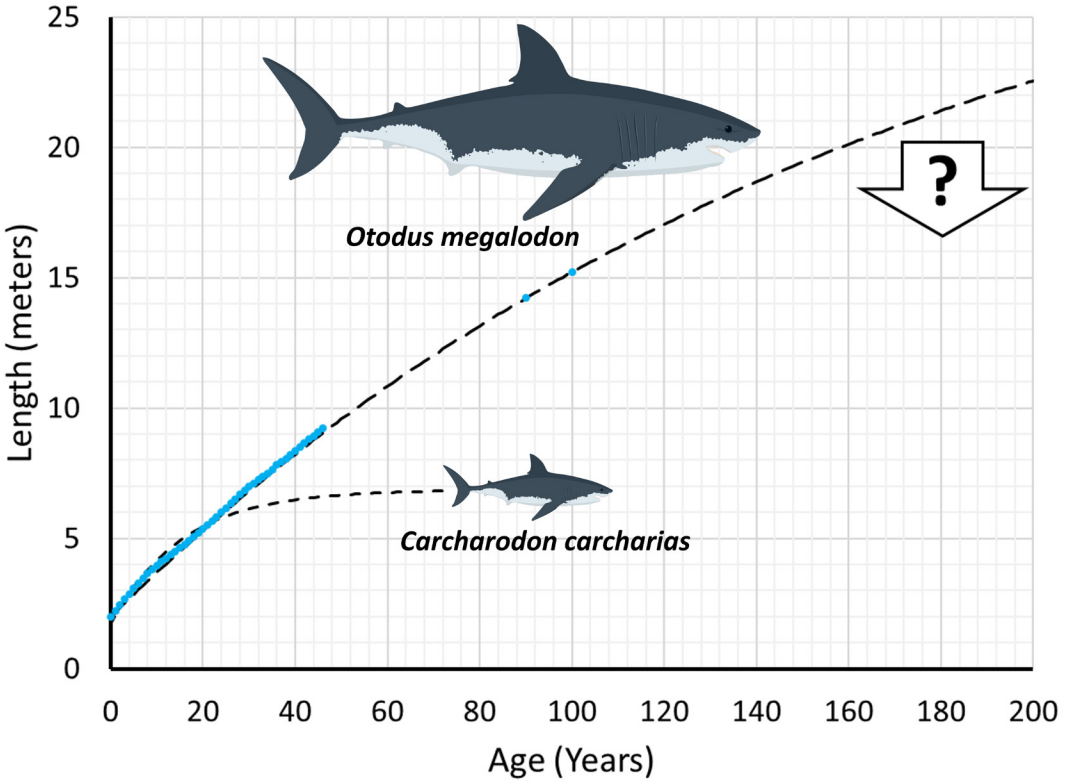

Figure 11. Length-versus-age data (light blue dots) inferred from *Otodus megalodon* teeth and vertebrae, as well as the extrapolated growth curve (dashed line), after Figure 2a in Shimada (2021). The specimen from which the vertebrae data were obtained had not yet matured, even though it is estimated to have been 46 years old at time of death. The great white shark growth curve of Wintner and Cliff (1999) is included for comparison. Shark image credit: Mostafa Elturkey. Wikimedia Commons, public domain.

still an adolescent, so to speak, and apparently had not yet reached its maximum size!

One particular extant shark, the Greenland shark, *Somniosus microcephalus*, is also very long-lived, with lifespans of 250-400 (and perhaps 500) years. This longevity is generally thought to be due to a very slow metabolism resulting from the cold waters in which it lives (Nielsen et al. 2016, O'Conner 2017). The Greenland shark is also one of the largest extant sharks and is thought to take 150 years to reach maturity. Both its large size and stretched-out growth interval are consistent with the trends noted in Section VB linking greater longevity in extant animals to greater adult size and longer growth periods.

However, cold temperatures seem inadequate to explain the apparent great longevity of these fossil sharks. Evolutionists think the Cretaceous climate was warm, and some creationists (Whitcomb and Morris 1991) have long suggested that the pre-Flood world was generally warmer than today's world, with presumably warmer oceans. Moreover, Cretaceous strata were deposited during the Flood, with much warmer oceans due to intense volcanism (Oard 1990) and rapid seafloor spreading (Baumgardner 1990). So both creationists and evolutionists would agree that the oceans in which these sharks swam were warm, albeit for different reasons. Moreover, evolutionists think megalodons lived in temperate-tropical waters (Shimada 2021), and creationists (at least those holding to a "high" Flood/post-Flood boundary) would argue that Miocene strata were also deposited during the Flood. Hence Miocene oceans should have been warm, as well. Yet despite living in temperate-to-warm waters, these fossil sharks demonstrate characteristics indicative of extreme longevity.

D. What about dinosaurs?

Of course, one cannot help but wonder about the largest of all land animals, the sauropod dinosaurs (Figure 12). Could their very large sizes be clues of great longevity, as suggested by Clarey (2018) and others? Paleontologists have used dinosaur osteo-histological data to construct growth curves for sauropods, as well as for other dinosaurs. However, as dinosaurs are extinct, ontogenetic growth curves for extant dinosaurs are rather difficult to come by! Hence, it is not possible to make a direct comparison of pre-Flood and post-Flood dinosaur growth rates and sizes.

Figure 12. Since reptiles have (apparently) indeterminate growth, could the large sizes of some sauropod dinosaurs be evidence of extreme longevity in the pre-Flood animal kingdom? Image credit: Video capture from *Uncovering the Truth About Dinosaurs,* Institute for Creation Research, Dallas, Texas. Used with permission.

However, given that large-mass animal kinds tend to live longer than lower-mass animal kinds, one would expect pre-Flood sauropod dinosaurs to have very long life spans and slow growth rates. However, most dinosaurian growth curves suggest that sauropod dinosaurs grew very rapidly (Sander 2000), with a peak *Apatosaurus* growth rate of 5,000 kg/year (Erickson et al. 2001). Such a high rate implies that Apatosaurus would have been a full-grown adult in just 15 years, contrary to expectations if its large size is indicative of slow growth and great longevity. However, in an extensive survey Myhrvold (2013) made astute criticisms of nearly *all* such constructed dinosaur growth curves, citing methodological and statistical fallacies or an inability to replicate the results. The only sauropod dinosaur growth curves he did not criticize were those of Woodward (2005) and Lehman and Woodward (2008), which implied much more modest peak sauropod growth rates of 520 kg/year for the *Apatosaurus* and 1,000 kg/year for *Alamosaurus.* With these lower rates, an *Apatosaurus* would need 70 years to reach maturity, as opposed to the 15 years estimated by Erickson et al. *Alamosaurus* would have needed 45 years to reach full size. However, Myhrvold cautioned that, even in those cases, the largest sauropod dinosaur was only 37% of its estimated adult size. Hence, in the case of sauropod dinosaurs, firm conclusions about total time to skeletal maturity and/or growth rate are probably as of yet unwarranted.

VI. CONLUDING REMARKS

Living things are vastly more complicated than imagined by Darwin. Hence it makes perfect sense that optimization methods such as Lagrange multipliers and impedance matching would be required to understand them. Although the WBE theory is probably not the final word in this area, it is a great starting point for those hoping to construct a creation-based theory of biological design, and it or a similar theory, such as that of Escala (2022), may help shed light on giantism and longevity in the pre-Flood worlds.

This paper included some paleontological speculation. Paleontology is outside my area of expertise, and I recognize my need for assistance in this area. However, creationists do not yet have a robust defense of the great longevity experienced by pre-Flood humans. Sadly, even many "evangelical" seminary professors are openly doubting the Bible's claims in this matter (Olson 2017, Olson ND, and discussion in Smith 2022). The possibility that paleontological data could help confirm that this longevity was shared by at least some pre-Flood animals is exciting, and I felt an urgent need to present it here at least as a possibility. For this reason, I appeal to creationist paleontologists, biologists, and statisticians to begin an aggressive and rigorous study of sclerochronological and paleo-osteo-histological data to see if a strong case can be made that pre-Flood animals were indeed attaining great ages compared to their extant counterparts.

REFERENCES

Abele, D., J. Strahl, T. Brey, and E. Philipp. 2008. Imperceptible senescence: ageing in the ocean quahog *Arctica islandica*. *Free Radical Research* 42, no. 5:474-480. DOI: 10.1080/10715760802108849.

Anonymous. Giant 'teenager' shark from the dinosaur era identified

from vertebrae remains. Retrieved April 25, 2023 from https://phys.org/news/2020-04-giant-teenager-shark-dinosaur-era.html.

Auer, S. K., K. Salin, A. M. Rudolf, G. J. Anderson, and N. B. Metcalfe. 2015. The optimal combination of standard metabolic rate and aerobic scope for somatic growth depends on food availability. *Functional Ecology* 29, no. 4:479-486. DOI: 10.1111/1365-2435.12396.

Ayala, F. J. 2007. Darwin's greatest discovery: Design without a designer. *Proceedings of the National Academy of Sciences* 104, suppl. 1:8567-8573. DOI: 10.1073/pnas.0701072104.

Baumgardner, J. R. 1990. 3-D element simulation of the global tectonic changes accompanying Noah's flood. In R. E. Walsh, and C. L. Brooks (editors), *Proceedings of the Second International Conference on Creationism*, pp. 35-44. Pittsburgh, Pennsylvania: Creation Science Fellowship.

Baxter-Gilbert, J., J. L. Riley, C. Wagener, N. P. Mohanty, and J. Measey. 2020. Shrinking before our isles: the rapid expression of insular dwarfism in two invasive populations of guttural toad (*Sclerophrys gutturalis*). *Biology Letters* 16, no. 11:1-6. DOI: 10.1098/rsbl.2020.0651.

Beasley, G. 1990. Pre-flood giantism: a key to the interpretation of fossil hominids and hominoids. *Journal of Creation* 4, no.1:5-55.

Bentley, L. P., J. C. Stegen, V. M. Savage, D. D. Smith, E. I. von Allmen, J. S. Sperry, P. B. Reich, and B. J. Enquist. 2013. An empirical assessment of tree branching networks and implications for plant allometric scaling models. *Ecology Letters* 16, no. 8:1069-1078. DOI: 10.1111/ele.12127.

Bergmann, C. 1847. *Ueber die verhältnisse der w*ärmeökonomie *der thiere zu ihrer grösse*, or *On the relationship between the heat economy of animals and their size*. Göttinger Stud. 3:595-708.

Brody, S. 1945. *Bioenergetics and Growth*. New York: Reinhold Publishing Corporation.

Brody, S., W. C. Hall, A. C. Ragsdale, E. A. Trowbridge, E. M. Funk, H. L. Kempster, U. S. Ashworth, A. G. Hogan, and R. C. Procter. 1932. Growth and development with specific reference to domesticated animals. XVII – XXIII. *University of Missouri Research Bulletin* 166:1-101.

Brown, J. H., G. B. West, and B. J. Enquist. 2000. Scaling in biology: Patterns and processes, causes and consequences. In J. H. Brown and G. B. West (editors), *Scaling in Biology*, pp. 1-24. Oxford: Oxford University Press.

Brown, J. H., G. B. West, and B. J. Enquist. 2005. Yes, West, Brown and Enquist's model of allometric scaling is both mathematically correct and biologically relevant. *Functional Ecology* 19, no. 4:735-738. DOI: 10.1111/j.1365-2435.2005.01022.x.

Buick, D. P. and L. C. Ivany. 2004. 100 years in the dark: Extreme longevity of Eocene bivalves from Antarctica. *Geology* 32, no. 10:921-924. DOI: 10.1130/G20796.1.

Calder, W. A. III. 1984. *Size, Function, and Life History*. Cambridge, Massachusetts: Harvard University Press.

Caro, C. G., T. J. Pendley, R. C. Schroter, and W. A. Seed. 2012. *The Mechanics of the Circulation*, 2nd edition. Cambridge: Cambridge University Press.

Chabreck, R. H. and T. Joanen. 1979. Growth rates of American alligators in Louisiana. *Herpetologica* 35, no. 1:51-57.

Chiappe, L. M. and A. Bell. 2020. *Mesozoic Birds*, eLS, Vol. 1: 549-557. DOI: 10.1002/9780470015902.a00292218.

Clarey, T. 2018. *Dinosaurs: Marvels of God's Design* (second printing). Green Forest, Arkansas: Master Books.

Clarey, T. L. 2019. South Caspian Basin supports a late Cenozoic Flood boundary. *Journal of Creation* 33, no. 3:8-11.

Cuozzo, J. 1998a. What happens to the craniofacial structures of humans who live past 100 years? Neanderthal similarities. In R. E. Walsh (editor), *Proceedings of the Fourth International Conference on Creationism*, pp. 103-119. Pittsburgh, Pennsylvania: Creation Science Fellowship.

Cuozzo, J. 1998b. *Buried Alive: The Startling Truth About Neanderthal Man*. Green Forest, Arkansas: Master Books.

Dawkins, R. 1986. *The Blind Watchmaker*. London: W. W. Norton & Company.

de Magalhães, J. P., J. Costa, and G. M. Church. 2007. An analysis of the relationship between metabolism, developmental schedules, and longevity using phylogenetic independent contrasts. *The Journals of Gerontology: Series A* 62, no. 2:149-160. DOI: 10.1093/Gerona/62.2.149.

Dillow, J. C. 1982. *The Waters Above: Earth's Pre-Flood Vapor Canopy* (revised edition). Chicago: Moody Press.

Dodds, P. S., D. H. Rothman, and J. S. Weitz. 2001. Re-examination of the "3/4-law" of metabolism. *Journal of Theoretical Biology* 209, no. 1:9-27. DOI: 10.1006/jtbi.2000.2238.

Enking, M. 2022. The World's Tallest Tree is Officially Off-Limits. Retrieved December 21, 2022 from https://www.smithsonianmag.com/smart-news/the-worlds-tallest-tree-is-officially-off-limits-180980509/.

Enquist, B. J., G. B. West, and J. H. Brown. 2000. Quarter-power allometric scaling in vascular plants: Functional basis and ecological consequences. In J. H. Brown and G. B. West (editors), *Scaling in Biology*, pp. 167-198. Oxford: Oxford University Press.

Enquist, B. J. and K. J. Niklas. 2001. Invariant scaling relations across tree-dominated communities. *Nature* 410, no. 6829:655-660. DOI: 10.1038/35070500.

Erickson, G. M. and G. A. Brochu. 1999. How the 'terror crocodile' grew so big. *Nature* 398, no. 6724:205-206. DOI: 10.1038/18343.

Erickson, G. M., K. C. Rogers, and S. A. Yerby. 2001. Dinosaurian growth patterns and rapid avian growth rates. *Nature* 412, no. 6845:429-433. DOI: 10.1038/35086558.

Erickson, G. M., O. W. M. Rauhut, Z. Zhou, A. H. Turner, B. D. Inouye, D. Hu, and M. A. Norell. 2009. Was dinosaurian physiology inherited by birds? Reconciling slow growth in *Archaeopteryx*. *PLoS ONE* 4, no. 10:1-9. DOI: 10.1371/journal.pone.0007390.

Escala, A. 2019. The principle of similitude in biology: From allometry to the formulation of dimensionally homogenous 'laws'. *Theoretical Ecology* 12, no. 4:415-425. DOI: 10.1007/s12080-019-0408-5.

Escala, A. 2021. Universal ontogenetic growth without fitted parameters: Implications for life history invariants and population growth. bioRχiv preprint. DOI: 10.1101/2021.10.10.463814. Retrieved May 13, 2023 from https://www.biorxiv.org/content/10.1101/2021.10.10.463814v2.full.pdf+html.

Escala, A. 2022. Universal relation for life-span energy consumption in living organisms: Insights for the origin of aging. *Scientific Reports* 12, no. 1:2407-2414. DOI: 10.1038/s41598-022-06390-6.

Etienne, R. S., M. E. F. Apol, and H. Olff. 2006. Demystifying the West, Brown & Enquist model of the allometry of metabolism. *Functional Ecology* 20, no. 2:394-399. DOI: 10.1111/j.1365-2435.2006.01136.x.

Feduccia, A. 2006. Mesozoic aviary takes form. *Proceedings of the National Academy of Sciences* 103, no. 1: 5-6. DOI: 10.1073/pnas.0509970102.

Foth, C., S. Wang, F. Spindler, Y. Lin, and R. Yang. 2021. A juvenile

specimen of *Archaeorhynchus* sheds new light on the ontogeny of basal Euornithines. *Frontiers in Earth Science* 9, no. 604520:1-19. DOI: 10.3389/feart.2021.604520.

Galileo Galilei. 1638. *Discorsi e Dimostrazioni Matematiche, Intorno à Due Nuoue Scienze*, or *The Discourses and Mathematical Demonstrations Relating to Two New Sciences*. Leiden, The Netherlands: House of Elzevir.

Gehr, P., D. K. Mwangi, A. Ammann, G. M. O. Maloiy, C. R. Taylor, E. R. Weibel. 1981. Design of the mammalian respiratory system. V. Scaling morphometric pulmonary diffusing capacity to body mass: Wild and domestic animals. *Respiratory Physiology* 44, no. 1:61-86. DOI: 10.1016.0034-5687(81)90077-3.

Genade, T., M. Benedetti, E. Terzibasi, P. Roncaglia, D. R. Valenzano, A. Cattaneo, and A. Cellerino. 2005. Annual fishes of the genus *Nothobranchius* as a model system for aging research. *Aging Cell* 4, no. 5:223-233. DOI: 1111/j.1474-9726.2005.00165.x.

Glazier, D. S. 2006. The ¾-power law is not universal: Evolution of isometric, ontogenetic metabolic scaling in pelagic animals. *Bioscience* 56, no. 4:325-332. DOI: 10.1641/0006-3568(2006)56[325:TPLINU]2.0.CO;2.

Godfrey-Smith, P. 2015. The ant and the steam engine. *London Review of Books* 37, no. 4 (February 19):18-20. Retrieved December 20, 2022 from https://www.lrb.co.uk/the-paper/v37/n04/peter-godfrey-smith/the-ant-and-the-steam-engine.

Greenhill, A.-G. 1881. Determination of the greatest height consistent with stability that a vertical pole or mast can be made, and of the greatest height to which a tree of given proportions can grow. *Proceedings of the Cambridge Philosophical Society*, vol. IV, part II:337-338. DOI: 10.1051/jphystap:018820010033701.

Guliuzza, R. J. 2017. Engineered adaptability: Engineering principles should guide biological research. *Acts & Facts* 46, no. 7 (July):17-19.

Guliuzza, R. J. and P. B. Gaskill. 2018. Continuous Environmental Tracking: An Engineering Framework to Understand Adaptation and Diversification. In J. H. Whitmore (editor), *Proceedings of the Eighth International Conference on Creationism*, pp. 158-184. Pittsburgh, Pennsylvania: Creation Science Fellowship.

Günther, B. 1975. Dimensional analysis and theory of biological similarity. *Physiological Reviews* 55, no. 4:659-699. DOI: 10.1152/physrev.1975.55.4.659.

Haldane, J. B. S. 1927. On Being the Right Size. In J. B. S. Haldane, *Possible Worlds and Other Essays*, pp. 18-26. London: Chatto and Windus.

Hariharan, I. K., D. B. Wake, and M. H. Wake. 2016. Indeterminate growth: could it represent the ancestral condition? *Cold Spring Harbor Perspectives in Biology* 8, no. 2:1-17. DOI: 10.1101/cshperspect.a019174.

Harrison, J. F., A. Kaiser, and J. M. VandenBrooks. 2010. Atmospheric oxygen level and the evolution of insect body size. *Proceedings of the Royal Society B* 277, no. 1690:1937-1946. DOI: 10.1098/rspb.2010.0001.

Hebert, J. 2022. Book Review: *Scaling in Biology*. *Creation Research Society Quarterly* 59, no. 1:60-61.

Holt, J. P., E. A. Rhode, W. W. Holt, and H. Kines. 1981. Geometric similarity of aorta, venae cavae, and certain of their branches in mammals. *American Journal of Physiology* 241, no. 1:R100-R104. DOI: 10.1152/AJPREGU.1981.241.1.R100.

Holt, R. D. 1996. Evidence for a late Cainozoic Flood/post-Flood boundary. *Journal of Creation* 10, no. 1:128-167.

Hulbert, A. J. 2014. A sceptics view: "Kleiber's law" or the "¾ Rule" is neither a law nor a rule but rather an empirical approximation. *Systems* 2, no. 2:186-202. DOI: 10.3390/systems2020186.

Huxley, J. S. 1924. Constant differential growth-ratios and their significance. *Nature* 114, no. 2877:895-896. DOI: 10.1038/114895a0.

Huxley, J. S. and G. Teissier. 1936. Terminology of relative growth. *Nature* 137, no. 3471:780-781. DOI: 10.1038/137780b0.

Jacob, F. 1977. Evolution and tinkering. *Science* 196, no. 4295:1161–1166. DOI: 10.1126/science.860134.

Jambura, P. L. and J. Kriwet. 2020. Articulated remains of the extinct shark *Ptychodus* (Elasmobranchii, Ptychodontidae) from the upper Cretaceous of Spain provide insights into gigantism, growth rate and life history of ptychodontid sharks. *PLoS ONE* 15, no. 4:1-16. DOI: 10.1371/journal.pone.0231544.

Killam, D., T. A.-Najjar, and M. Clapham. 2021. Giant clam growth in the Gulf of Aqaba is accelerated compared to fossil populations. *Proceedings of the Royal Society* B 288, no. 1957:1-8. DOI: 10.1098/rspb.2021.0991.

Kirby, M. X. 2001. Differences in growth rate and environment between Tertiary and Quaternary *Crassostrea* oysters. *Paleobiology* 27, no. 1:84-103. DOI: 10.1666/0094-8373(2001)027<0084:DIGRAE>2.0.CO;2.

Kleiber, M. 1932. Body size and metabolism. *Hilgardia* 6, no. 11:315-353. DOI: 10.3733/hilg.v06n11p315.

Kleiber, M. 1947. Body size and metabolic rate. *Physiological Reviews* 27, no. 4:511-541. DOI: 10.1152/physrev.1947.27.4.511.

Kleiber, M. 1961. *The Fire of Life: An Introduction to Animal Energetics*. New York, John Wiley & Sons, Inc.

Korteweg, D. J. 1878. Über die Fortpflanzungsgeschwindigkeit des Schalles in Elastischen Röhren, or On the speed of propagation of sound in elastic tubes. *Annalen der Physik* 241, no. 12: 525-542. DOI: 10.1002/andp.18782411206.

Kozłowski, J. and M. Konarzewski. 2004. Is West, Brown and Enquist's model of allometric scaling mathematically correct and biologically relevant? *Functional Ecology* 18, no. 2:283-289.

Kozłowski, J. and M. Konarzewski. 2005. West, Brown and Enquist's model of allometric scaling again: the same questions remain. *Functional Ecology* 19, no. 4:739-743. DOI: 10.1111/j.1365-2435.2005.01021.x.

Lee, W.-S., P. Monaghan, and N. B. Metcalfe. 2013. Experimental demonstration of the growth rate-lifespan trade-off. *Proceedings of the Royal Society B* 280:1-8. DOI: 10.1098/rspb.2012.2370.

Lehman, T. M. and H. N. Woodward. 2008. Modeling growth rates for sauropod dinosaurs. *Paleobiology* 34, no. 2:264-281. DOI: 10.1666/0094-8373(2008)034[0264:MGRFSD]J2.0.CO;2.

Li, J. K-J. 2000. Scaling and invariants in cardiovascular biology. In J. H. Brown, and G. B. West (editors), *Scaling in Biology*, pp. 113-128. Oxford: Oxford University Press.

Lindstedt, S. 1981. Body size, physiological time, and longevity of homeothermic animals. *The Quarterly Review of Biology* 56, no. 1:1-16. DOI: 10.1086/412080.

Line, P. 2013. Explaining robust humans. *Journal of Creation* 27, no. 3:64-71.

Lomolino, M. V. 2005. Body size evolution in insular vertebrates: generality of the island rule. *Journal of Biogeography* 32, no. 10:1683-1699. DOI: 10.1111/j.1365-2699.2005.01314.x.

Lubenow, M. L. 2004. *Bones of Contention: A Creationist Assessment of Human Fossils* (revised and updated edition). Grand Rapids, Michigan: Baker Books.

Marchionni, S., C. Sell, and A. Lorenzini. 2020. Development and longevity: Cellular and molecular determinants – a mini-review. *Gerontology* 66, no.

3:223-230. DOI: 10.1159/00050505327.

McMahon, T. A. and J. T. Bonner. 1983. *On Size and Life*. New York: Scientific American Books.

Miller, B. 2022. The surprising relevance of engineering in biology. *Dallas Conference on Science & Faith.* Denton, Texas. Retrieved August 10, 2022, from https://www.youtube.com/watch?v=M9i2vFEa6rE.

Minamino, R. and M. Tateno. 2014. Tree branching: Leonardo da Vinci's rule versus biomechanical models. *PLoS ONE* 9, no. 4:1-12. DOI: 10.1371/journal.pone.0093535.

Moens, A. I. 1878. *Die Pulskurve*, or *The Pulse Curve*. Leiden, The Netherlands: E. J. Brill.

Moss, D. K., L. C. Ivany, E. J. Judd, P. W. Cummings, C. E. Bearden, W.- J. Kim, E. J. Artruc, and J. R. Driscoll. 2016. Lifespan, growth rate, and body size across latitude in marine Bivalvia, with implications for Phanerozoic evolution. *Proceedings of the Royal Society B* 283, no. 1836:1-7. DOI: 10.1098/rspb.2016.1364.

Moss, D. K., L. C. Ivany, R. B. Silver, J. Schue, and E. G. Artruc. 2017. High-latitude settings promote extreme longevity in fossil marine bivalves. *Paleobiology* 43, no. 3:365-382. DOI: 10.1017/pab.2017.5.

Moss, D. K., L. C. Ivany, and D. S. Jones. 2021. Fossil bivalves and the sclerochronological reawakening. *Paleobiology* 47, no. 4:1-23. DOI: 10.1017/pab.2021.16.

Murray, C. D. 1926. The physiological principle of minimum work. I. The vascular system and the cost of blood volume. *Proceedings of the National Academy of Sciences* 12, no. 3:207-214. DOI: 10.1073/pnas.12.3.207.

Myhrvold, N. P. 2013. Revisiting the estimation of dinosaur growth rates. *PLoS ONE* 8, no. 12:1-24. DOI: 10.1371/journal.pone.0081917.

Nelson, V. 2017. *Monumental Monsters*. Red Deer, Alberta, Canada: Untold Secrets of Planet Earth Publishing Company, Inc.

Nielsen, J., R. B. Hedeholm, J. Heinemeier, P. G. Bushnell, J. S. Christiansen, J. Olsen, C. B. Ramsey, R. W. Brill, M. Simon, K. F. Steffensen, and J. F. Steffensen. 2016. Eye lens radiocarbon reveals centuries of longevity in the Greenland shark (*Somniosus microcephalus*). *Science* 353, no. 6300:702-704. DOI: 10.1126/science.aaf1703.

Niklas, K. J. 1995. Size-dependent allometry of tree height, diameter and trunk-taper. *Annals of Botany* 75, no. 3:217-227. DOI: 10.1006/anbo.1995.1015.

Niklas, K. J. 1997. Size- and age-dependent variation in the properties of the sap- and heartwood in Black Locust (*Robinia pseudoacacia* L.). *Annals of Botany* 79, no. 5:473-478. DOI: 10.1006/anbo.1996.0354.

Niklas, K. J. 2004. Plant allometry: is there a grand unifying theory? *Biological Reviews* 79, no. 4:871-889. DOI: 10.1017/S1464793104006499.

Oard, M. J. 1990. *An Ice Age Caused by the Genesis Flood*. El Cajon, California. Institute for Creation Research.

Oard, M. J. 2002. Dealing carefully with the data. *Journal of Creation* 16, no. 1:68-72.

Oard, M. J. 2013. Geology indicates the terrestrial Flood/post-Flood boundary is mostly in the late Cenozoic. *Journal of Creation* 27, no. 1:119-127.

O'Connor, J., W. Min, Z. Xiao-Ting, W. Xiao-Li, and Z. Zhong-He. 2014. The histology of two female Early Cretaceous birds. *Vertebrata PalAsiatica* 52, no. 1:112-128.

O'Connor, M. R. 2017. The strange and gruesome story of the Greenland shark, the longest-living vertebrate on Earth. Retrieved May 15, 2023 from https://www.newyorker.com/tech/annals-of-technology/the-strange-and-gruesome-story-of-the-greenland-shark-the-longest-living-vertebrate-on-earth.

Olson, C. 2017. How old was Father Abraham? Re-examining the patriarchal lifespans in light of archaeology. Paper presented at the Southwest Regional Meeting of the Evangelical Theological Society (March 31-April 1): 1-26. Retrieved April 28, 2023, from https://www.academia.edu/33972456/How_Old_was_Father_Abraham_Re_examining_the_Patriarchal_Lifespans_in_Light_of_Archaeology.

Olson, C. No date. How old was Father Abraham? Part 2: A symbolic interpretation of the patriarchal lifespans: 1-28. Retrieved April 28, 2023, from https://www.academia.edu/44203083/How_Old_was_Father_Abraham_Part_2_A_Symbolic_Interpretation_of_the_Patriarchal_Lifespans

Padian, K. 2023. 25th anniversary of first feathered-dinosaur finds. *Nature* 613, no. 7943:251-252. DOI: 10.1038/d41586-022-04586-4.

Palmer, K. L., D. K. Moss, D. Surge, and S. Turek. 2021. Life history patterns of modern and fossil *Mercenaria* spp. from warm vs. cold climates. *Palaeogeography, Palaeoclimatology, and Palaeoecology* 566, no. 3: 110227. DOI: 10.1016/j.palaeo.2021.110227.

Pauly, D. and J. L. Munro. 1984. Once more on the comparison of growth in fish and invertebrates. *Fishbyte* 2, no. 1:1-21.

Peters, R. H. 1993. *The Ecological Implications of Body Size* (5th printing). Cambridge: Cambridge University Press.

Price, C. A., P. Drake, E. J. Veneklaas, and M. Renton. 2022. Flow similarity, stochastic branching, and quarter-power scaling in plants. *Plant Physiology* 190, no. 3:1854-1865. DOI: 10.1093/plphys/kiac358.

Price, C. A., S. Wing, and J. S. Weitz. 2011. Scaling and structure of dicotyledonous leaf venation networks. *Ecology Letters* 15, no. 2:87-95. DOI: 10.1111/j.1461-0248.2011.01712.x.

Prothero, J. W. 1980. Scaling of blood parameters in mammals. *Comparative Biochemistry and Physiology Part A* 67, no. 4:649-657. DOI: 10.1016/0300-9629(80)90255-8.

Ricklefs, R. E. 2010a. Life-history connections to rates of aging in terrestrial vertebrates. *Proceedings of the National Academy of Sciences* 107, no. 22:10314-10319. DOI: 10.1073/pnas.1005862107.

Ricklefs, R. E. 2010b. Embryo growth rates in birds and mammals. *Functional Ecology* 24, no. 3:588-596. DOI: 10.1111/j.1365-2435.2009.01684.x.

Ridgway, I. D., C. A. Richardson, and S. N. Austad. 2011. Maximum shell size, growth rate, and maturation age correlate with longevity in bivalve molluscs. *The Journals of Gerontology: Series A* 66A, no. 2:183-190. DOI: 10.1093/Gerona/glq172.

Roopnarine, P. D. 1996. Systematics, biogeography and extinction of chionine bivalves (Bivalvia: Veneridae) in tropical America: Early Oligocene-Recent. *Malacologia* 38, no. 1-2:103-142.

Rupe, C. and J. Sanford. 2017. *Contested Bones*. FMS Publications.

Sander, P. M. 2000. Longbone histology of the Tendaguru sauropods: Implications for growth and biology. Paleobiology 26, no. 3:466-488.

Sato, S. 1999. Temporal change of life-history traits in fossil bivalves: an example of *Phacosoma japonicum* from the Pleistocene of Japan. *Palaeogeography, Palaeoclimatology, Palaeoecology* 154, no. 4:313-323. DOI: 10.1016/S0031-0182(99)00106-6.

Savage, V. M., E. J. Deeds, and W. Fontana. 2008. Sizing up allometric scaling theory. *PLOS Computational Biology* 4, no. 9:1-17. DOI: 10.1371/journal.pcbi.1000171.

Schmidt-Nielsen, K. 1986. *Scaling: Why Is Animal Size So Important?* (3rd

printing). Cambridge: Cambridge University Press.

Seebacher, F. 2001. A new method to calculate allometric length-mass relationships of dinosaurs. *Journal of Vertebrate Paleontology* 21, no. 1:51-60. DOI: 10.1671/0272-4634(2001)021[0051:ANMTCA]2.0.CO;2.

Sereno, P. C., H. C. E. Larsson, C. A Sidor, and B. Gado. 2001. The giant crocodyliform *Sarcosuchus* from the Cretaceous of Africa. *Science* 294, no. 5546:1516-1519. DOI: 10.1126/science.1066521.

Shimada, K., M. J. Everhart, R. Decker, and P. D. Decker. 2010. A new skeletal remain of the durophagous shark, *Ptychodus mortoni*, from the Upper Cretaceous of North America: an indication of gigantic body size. *Cretaceous Research* 31, no. 2:249-254. DOI: 10.1016/j.cretres.2009.11.005.

Shimada, K., M. F. Bonnan, M. A. Becker, and M. L. Griffiths. 2021. Ontogenetic growth pattern of the extinct megatooth shark *Otodus megalodon* – implications for its reproductive biology, development, and life expectancy. *Historical Biology* 33, no. 12:3254-3259. DOI: 10.1080/08912963.2020.1861608.

Shirazi, M. 1972. Theory of Arterial Circulation. Wright-Patterson Air Force Base, OH: United States Aerospace Medical Research Laboratory.

Smith, H. B. 2022. Wild West hermeneutics, Part 3: The patriarchal life spans. *Bible and Spade* 35, no. 3-4:42-52.

Spiegel, M. R. 1994. *Schaum's Outline Series: Mathematical Handbook of Formulas and Tables*. New York: McGraw-Hill.

Stahl, W. R. 1967. Scaling of respiratory variables in mammals. *Journal of Applied Physiology* 22, no. 3: 453-460. DOI: 10.1152/jappl.1967.22.3.453.

Tenney, S. M. and D. Bartlett, Jr. 1967. Comparative quantitative morphology of the mammalian lung: Trachea. *Respiratory Physiology* 3, no. 2:130-135. DOI: 10.1016.0034-5687(67)90002-3.

Thomas, G. B., Jr. and R. L. Finney. 1988. *Calculus and Analytic Geometry*, 7th edition. Reading, Massachusetts: Addison-Wesley Publishing Company.

Thompson, D. W. 1917. *On Growth and Form*. London: Cambridge University Press.

Tomkins, J. P. 2019. Recent humans with archaic features upend evolution. *Acts & Facts* 48, no. 4 (April): 15.

Tredennick, A. T., L. P. Bentley, and N. P. Hanan. 2013. Allometric convergence in savanna trees and implications for the use of plant scaling models in variable ecosystems. *PLOS ONE* 8, no. 3:1-11. DOI: 10.1371/journal.pone.0058241.

von Bertalanffy, L. 1938. A quantitative theory of organic growth (inquiries on growth laws II). *Human Biology* 10, no. 2:181-213. DOI: Weibel, E. R. 1972. Morphometric estimation of pulmonary diffusion capacity. V. Comparative morphometry of alveolar lungs. *Respiration Physiology* 14, no. 1:26-43. DOI: 10.1016/0034-5687(72)90015-1.

Weibel, E. R. 1972. Morphometric estimation of pulmonary diffusion capacity. V. Comparative morphometry of alveolar lungs. *Respiration Physiology* 14, no. 1:26-43. DOI: 10.1016/0034-5687(72)90015-1.

West, G. B. and J. H. Brown. 2005. The origin of allometric scaling laws in biology from genomes to ecosystems: towards a quantitative unifying theory of biological structure and organization. *The Journal of Experimental Biology* 208, no. 9:1575-1592. DOI: 10.1242/jeb.01589.

West, G. B., J. H. Brown, and B. J. Enquist. 1997. A general model for the origin of allometric scaling laws in biology. *Science* 276, no. 5309:122-126. DOI: 10.1126/science.276.5309.122

West, G. B., J. H. Brown, and B. J. Enquist. 2000. The origin of universal scaling laws in biology. In J. H. Brown and G. B. West (editors), *Scaling in Biology*, pp. 87-112. Oxford: Oxford University Press.

West, G. B., J. H. Brown, and B. J. Enquist. 2001. A general model for ontogenetic growth. *Nature* 413, no. 6856:628-631. DOI: 10.1038/35098076.

Whitcomb, J. C. and H. M. Morris. 1991. *The Genesis Flood: The Biblical Record and Its Scientific Implications* (35th printing). Phillipsburg, New Jersey: Presbyterian & Reformed Publishing Company.

White, C. R. and R. S. Seymour. 2003. Mammalian basal metabolic rate is proportional to body mass$^{2/3}$. *Proceedings of the National Academy of Sciences* 100, no. 7:4046-4049. DOI: 10.1073/pnas.0436428100.

White, C. R. and R. S. Seymour. 2005. Review: Allometric scaling of mammalian metabolism. *The Journal of Experimental Biology* 208, no. 9:1611-1619. DOI: 10.1242/jeb.01501.

Wieland, C. and J. D. Sarfati. 2011. Some bugs do grow bigger with higher oxygen. *Journal of Creation* 25, no. 1:13-14.

Wintner, S P. and G. Cliff. 1999. Age and growth determination of the white shark, *Carcharodon carcharias*, from the east coast of South Africa. *Fishery Bulletin* 97, no. 1:153-169.

Womersley, J. R. 1955. Method for the calculation of velocity, rate of flow and viscous drag in arteries when the pressure gradient is known. *Journal of Physiology* 127, no. 3:553-563. DOI: 10.1113/jphysiol.1955.sp005276.

Woodward, H. 2005. *Bone histology of the sauropod dinosaur Alamosaurus sanjuanensis from the Javelina Formation, Big Bend National Park, Texas* [masters thesis]. Lubbock, Texas: Texas Tech University.

APPENDIX A: Optimization for Narrow Blood Vessels

These derivations are included as "guideposts" to other researchers, as details of the derivations are not always clearly or succinctly explained in the literature. Appendices A through C primarily follow the methodology of Savage et al. (2008), as they include details omitted in the overview provided by WBE.

For a fluid with viscosity μ the Hagen-Poiseuille formula gives the hydrodynamic resistance R to laminar, steady fluid flow in a short pipe of length l and radius r. One may derive the Hagen-Poiseuille expression by solving the Navier-Stokes equation (in cylindrical coordinates r, z, and ϕ) for steady-state (no time dependence, and no z-dependence of velocity upon position) laminar flow of an incompressible fluid in a short, azimuthally symmetric pipe. The fluid undergoes motion in only the z-direction and is subject to the boundary condition that fluid velocity at the pipe wall ($r = R$) is zero. Solving this equation in cylindrical coordinates yields an expression for Δp in terms of current velocity $w(r)$ in the z-direction. Averaging this over the cross-sectional area of the pipe yields an expression for the volume current flow $\dot{Q}$:

$$\Delta p = \frac{8\mu l \dot{Q}}{\pi r^4} = \dot{Q}R \tag{A1}$$

Physicists and electrical engineers will note the similarity between Eq. (A1) and the equation $\Delta V = IR$. Hence the expression for the hydrodynamic resistance R is

$$R = \frac{8\mu l}{\pi r^4} \tag{A2}$$

For a hierarchical fluid distribution network with $N + 1$ levels of

pipes, the total resistance of the network is the sum of the resistances of each level of the network, just as the equivalent resistance of electrical resistors in series is equal to the sum of the individual resistances:

$$R_{network} = \sum_{k=0}^{N} R_{\text{level } k} \tag{A3}$$

Each level has $N_k = n^k$ identical pipes of length l_k and radius r_k. Hence, each level of the network has n^k hydrodynamic resistances in parallel with one another. Eq. (A3) becomes

$$R_{network} = \sum_{k=0}^{N} R_{\text{level } k} = \sum_{k=0}^{N} \frac{R_k}{N_k} = \sum_{k=0}^{N} \frac{8\mu l_k}{n^k \pi r_k^4} \tag{A4}$$

If a total current $\dot{Q}_0$ flows through the network, the total power dissipated is

$$P_{loss} = \dot{Q}_0^2 R_{network} \tag{A5}$$

The method of Lagrange multipliers (Thomas and Finney 1988) is used to find the parameters that minimize this power loss, assuming that the organism's mass M, blood volume V_b, and products $N_k l_k^3 \propto V$ are known quantities. The method requires the construction of an 'auxiliary function' F' that is a function of the variables allowed to vary in order to minimize the power loss, i.e., r_k, l_k, and n, as well as the undetermined multipliers λ_b', λ_M', and the λ_k':

$$F'(r_k, l_k, n, \lambda_b', \lambda_M', \lambda_0', \lambda_1', \ldots, \lambda_N') = P_{loss}(r_k, l_k, n, M) + \lambda_b' V_b(r_k, l_k, n, M) + \lambda_M' M + \sum_{k=0}^{N} \lambda_k' N_k l_k^3$$
$$= \dot{Q}_0^2 \sum_{k=0}^{N} \frac{8\mu l_k}{n^k \pi r_k^4} + \lambda_b' \sum_{k=0}^{N} n^k (\pi r_k^2 l_k) + \lambda_M' M + \sum_{k=0}^{N} \lambda_k' n^k l_k^3 \tag{A6}$$

Note that the volume filling constraint has been applied $N+1$ times, because it must hold for all $N+1$ levels of the network. The equation for the volume of a cylinder was used to obtain an expression for the total volume of blood V_b within the network. As noted in the Supplementary Materials section of Savage et al (2008), this expression may be simplified considerably since μ, π, and $\dot{Q}_0^2$ are constants:

$$F(r_k, l_k, n, \lambda_b, \lambda_M, \lambda_0, \lambda_1, \ldots, \lambda_N) = \sum_{k=0}^{N} \frac{l_k}{n^k r_k^4} + \lambda_b \sum_{k=0}^{N} n^k (\pi r_k^2 l_k) + \lambda_M M + \sum_{k=0}^{N} \lambda_k n^k l_k^3 \tag{A7}$$

An optimizing expression for r_k is obtained by taking the partial derivatives of F with respect to r_k and setting that partial derivative equal to 0:

$$\frac{\partial F}{\partial r_k} = 0 = \sum_{k=0}^{N} \frac{-4 l_k}{n^k r_k^5} + \lambda_b \sum_{k=0}^{N} n^k (2\pi r_k l_k) \tag{A8}$$

Since λ_b must be independent of k, one may be tempted to solve for λ_b directly:

$$\lambda_b = \frac{\sum_{k=0}^{N} \frac{4 l_k}{n^k r_k^5}}{\sum_{k=0}^{N} n^k (2\pi r_k l_k)} \tag{A9}$$

But it is *much* easier to observe that Eq. (A8) is also satisfied if

$$\lambda_b = \frac{2}{\pi (n^{2k} r_k^6)} \tag{A10}$$

and one then imposes the constraint that λ_b be independent of k:

$$n^{2k} r_k^6 = n^{2(k+1)} r_{k+1}^6 \tag{A11}$$

This implies that

$$\frac{r_{k+1}}{r_k} = n^{-\frac{1}{3}} = \beta_k = \beta_>, \tag{A12}$$

where we have introduced the symbol $\beta_>$ to show that this constraint applies for narrow blood vessels, denoted by k values greater than some particular $k = \bar{k}$. Taking the partial derivative of F with respect to l_k and setting the derivative equal to 0 leads to the "volume filling" requirement obtained in Section IIIB:

$$\frac{l_{k+1}}{l_k} = n^{-\frac{1}{3}} = \gamma_k = \gamma \tag{A13}$$

One may then show that the first and fourth terms (which are themselves sums) on the right-hand-side of Eq. (A7) add to zero. This results in a simplified expression for F:

$$F = \lambda_b V_b + \lambda_M M \tag{A14}$$

Since F does not depend on mass M, differentiating Eq. (A14) with respect to M yields

$$0 = \lambda_b \frac{\partial V_b}{\partial M} + \lambda_M \tag{A15}$$

Integrating Eq. (A15) and imposing the requirement that $V_b = 0$ when $M = 0$ implies that

$$V_b \propto M \tag{A16}$$

Eq. (A16) plays an important role in deriving Kleiber's Law, as shown in Appendix C.

APPENDIX B: OPTIMIZATION FOR WIDE BLOOD VESSELS

The smaller surface area to volume ratio found in thicker blood vessels implies that dissipation due to wave reflection at node junctions is a much greater source of power loss than friction. This power loss may (in theory) be completely eliminated via the process of impedance matching. This discussion follows the methodology of Savage et al. (2008) and Caro et al. (2012).

Pressure in the arterial system consists of both steady-state and oscillatory components (Caro et al. 2012). Since the steady-state components do not change, it is sufficient to consider just the oscillatory incident, reflected, and transmitted pressure and current waveforms:

$$\begin{matrix} p_i e^{i(\kappa_1 x-\omega t)} & \dot{Q}_i e^{i(\kappa_1 x-\omega t)} \\ p_r e^{i(-\kappa_1 x-\omega t)} & \dot{Q}_r e^{i(-\kappa_1 x-\omega t)} \\ p_t e^{i(\kappa_2 x-\omega t)} & \dot{Q}_t e^{i(\kappa_2 x-\omega t)} \end{matrix} \quad \text{(B1)}$$

Note that the additional minus sign in the expressions in the second row of Eq. (B1) take into account the fact that the reflected waves propagate in the direction opposite to the incident waves. Also, the incident and reflected wave numbers are both denoted by κ_1, since wavenumber is a property of the artery and not the wave itself. Here, the currrent amplitudes are positive real numbers, but the pressure amplitudes are complex, with the complex parts of each current incorporated into each (complex) pressure amplitude. This allows for possible phase differences between waveforms. At the node junction ($x = 0$) and at all times t, the sum of the incident and reflected waves must equal that of the transmitted wave:

$$p_i + p_r = p_t \quad \text{(B2)}$$

If this were not the case, then any existing pressure difference would quickly drive blood toward the region of lower pressure, removing the pressure difference.

Impedance Z is defined as the ratio of applied oscillatory pressure to resulting oscillatory fluid flow. It is a property of the blood vessel and not the wave *per se*. Hence, the expressions relating the incident and reflected pressure waveforms to their corresponding currents will both be expressed in terms of the same impedance Z_k, and the transmitted wave will be expressed in terms of the impedance Z_{k+1}. The pressure and current amplitudes are related by

$$\begin{aligned} p_i &= Z_k \dot{Q}_i \\ p_r &= Z_k \dot{Q}_r \\ p_t &= Z_{k+1} \dot{Q}_t \end{aligned} \quad \text{(B3)}$$

Since the pressure amplitudes may generally be complex, the impedances may be complex, as well. At all times, the net inbound current at the junction must equal the outbound current, so

$$\dot{Q}_i - \dot{Q}_r = n\dot{Q}_t \quad \text{(B4)}$$

Substituting the expressions from Eq. (B3) into Eq. (B4) yields

$$\frac{p_i}{Z_k} - \frac{p_r}{Z_k} = n\frac{p_t}{Z_{k+1}} \quad \text{(B5)}$$

Adding together and then subtracting Eqs. (B2) and (B5) results in an expression for the reflected pressure amplitude in terms of the incident pressure amplitude:

$$p_r = \frac{Z_{k+1} - nZ_k}{Z_{k+1} + nZ_k} p_i \quad \text{(B6)}$$

To minimize power losses, the reflected amplitude should be zero. This condition is met if

$$nZ_k = Z_{k+1} \quad \text{(B7)}$$

For the special case of inviscid (negligible viscosity) fluid flow, the hydrodynamic impedance is (Caro et al. 2012):

$$Z_k = \frac{c_0 \rho}{\pi r_k^2} \quad \text{(B8)}$$

where ρ is blood density and c_0 is the Korteweg-Moens velocity (Moens 1878; Korteweg 1878), the velocity at which a blood pressure pulse propagates through the arterial system when viscosity is negligible. Eqs. (B7) and (B8) imply that, for large blood vessels, impedance matching is achieved if

$$\frac{r_{k+1}}{r_k} = n^{-\frac{1}{2}} = \beta_k = \beta_<, \quad \text{(B9)}$$

where we have introduced the symbol $\beta_<$ to show that this constraint applies for wide blood vessels, denoted by k values less than some particular $k = \bar{k}$.

Appendix C: Derivation of Kleiber's Law

Obtaining a general expression for blood vessels of intermediate length is extraordinarily difficult (see Shirazi 1972), and we omit this discussion here. However, from the results of the previous two appendices, it is apparent that efficiency of the cardiovascular system is increased by using the volume-filling condition expressed in Eq. (A13), as well as Eq. (A12) for narrow blood vessels and Eq. (B9) for wide blood vessels, as shown in Figure 6. Here we derive Kleiber's Law, as illustrated by Savage et al. (2008). The total volume of fluid (here assumed to be blood) in the organism is equal to the total volume of the network:

$$V_b = \sum_{k=0}^{N} N_k\left(\pi r_k^2 l_k\right) = \sum_{k=0}^{N} n^k\left(\pi r_k^2 l_k\right) \quad \text{(C1)}$$

This sum may be partitioned into two parts, where $k = \bar{k}$ marks the transition between wide and narrow blood vessels:

$$V_b = \sum_{k=0}^{\bar{k}} n^k\left(\pi r_k^2 l_k\right) + \sum_{k=\bar{k}+1}^{N} n^k(\pi r_k^2 l_k) \quad \text{(C2)}$$

Since the volume-filling constraint holds for all values of k, we have

$$l_k = \gamma^k l_0 \quad \text{for all } k, \quad \text{(C3)}$$

and our generalized expression for the radius of each vessel is

$$r_k = \begin{cases} (\beta_<)^k r_0 & \text{for } k \le \bar{k} \\ (\beta_>)^{k-\bar{k}} (\beta_<)^{\bar{k}} r_0 & \text{for } k > \bar{k} \end{cases} \quad \text{(C4)}$$

where we have defined

$$\beta_k \equiv \begin{cases} \beta_< = n^{-\frac{1}{2}} & \text{for } k \le \bar{k} \\ B_> = n^{-\frac{1}{3}} & \text{for } k > \bar{k} \end{cases} \quad \text{(C5)}$$

Eqs. (C3) and (C4) imply that the volume of each capillary is

$$\begin{aligned} V_{cap} &= \pi r_N^2 l_N \\ &= \pi r_0^2 l_0 \left(\beta_>\right)^{2(N-\bar{k})} \left(\beta_<\right)^{2\bar{k}} \gamma^N \\ &= \pi r_0^2 l_0 (\beta_>)^{2N} \left(\frac{\beta_<}{\beta_>}\right)^{2\bar{k}} \gamma^N \end{aligned} \tag{C6}$$

The number of capillaries is

$$N_{cap} = n^N \tag{C7}$$

Inserting our expressions for $\beta_>$, $\beta_<$, γ and N_{cap} into Eq. (C6) gives

$$V_{cap} = \frac{(\pi r_0^2 l_0)}{N_{cap} n^{\frac{\bar{k}}{3}}} \tag{C8}$$

By making use of the formula for a geometric series (Spiegel 1994), the first sum in Eq. (C2) becomes

$$\begin{aligned} \sum_{k=0}^{\bar{k}} n^k \left(\pi r_k^2 l_k\right) &= \sum_{k=0}^{\bar{k}} (n\gamma\beta_<^2)^k (\pi r_0^2 l_0) \\ &= (\pi r_0^2 l_0) \sum_{k=0}^{\bar{k}} (n^{-1/3})^k = V_{cap} N_{cap} n^{\bar{k}/3} \frac{1-(n^{-1/3})^{\bar{k}+1}}{1-n^{-1/3}} \end{aligned} \tag{C9}$$

By defining $\bar{N} = N - \bar{k}$, the second expression in Eq. (C2) becomes

$$\begin{aligned} \sum_{k=\bar{k}+1}^{N} n^k \left(\pi r_0^2 l_0\right)(\beta_>)^{2(k-\bar{k})}(\beta_<)^{2\bar{k}} \gamma^k &= \left(\frac{\beta_<}{\beta_>}\right)^{2\bar{k}} (\pi r_0^2 l_0) \sum_{k=\bar{k}+1}^{N} (n\gamma\beta_>^2)^k = \left(\frac{\beta_<}{\beta_>}\right)^{2\bar{k}} (\pi r_0^2 l_0) \sum_{k=\bar{k}+1}^{N} 1^k \\ &= \left(\frac{\beta_<}{\beta_>}\right)^{2\bar{k}} (\pi r_0^2 l_0)(N-\bar{k}) \\ &= V_{cap} N_{cap} \bar{N} \end{aligned} \tag{C10}$$

Combining the expressions for these two sums and some algebra gives us the blood volume:

$$V_b = V_{cap} N_{cap} \left[\frac{N_{cap}^{\frac{1}{3}} n^{\frac{(1-\bar{N})}{3}} - 1}{n^{\frac{1}{3}} - 1} + \bar{N}\right] \tag{C11}$$

Remember that, according the first assumption of the WBE theory, the volume of a capillary V_{cap} is the same regardless of the mass of the organism. Hence, it is a mass-independent quantity. The same is true for the branching ratio n and the number $\bar{N}$. Thus the only mass-dependent variable on the right-hand side of Eq. (C11) is N_{cap}. Defining the mass-independent constants

$$C_0 = \frac{V_{cap} n^{\frac{(1-\bar{N})}{3}}}{n^{\frac{1}{3}} - 1} \quad \text{and} \quad C_1 = V_{cap}\left(\bar{N} - \frac{1}{n^{\frac{1}{3}} - 1}\right) \tag{C12}$$

gives us

$$V_b = C_0 N_{cap}^{\frac{4}{3}} + C_1 N_{cap} = C_0 N_{cap}^{\frac{4}{3}} \left(1 + \frac{C_1}{C_0} N_{cap}^{-\frac{1}{3}}\right) \tag{C13}$$

In Appendix A it was shown that body mass M is proportional to blood volume V_b. Therefore

$$M = A V_b = A C_0 N_{cap}^{\frac{4}{3}} \left(1 + \frac{C_1}{C_0} N_{cap}^{-\frac{1}{3}}\right) \tag{C14}$$

Intuitively, we expect the total basal metabolic rate B to equal the sum of the metabolic rates of the individual service volumes. Since there are N_{cap} such service volumes, $B \propto N_{cap}$, or equivalently, $N_{cap} \propto B$. So we have

$$M = A_0 B^{\frac{4}{3}} \left(1 + A_1 B^{-\frac{1}{3}}\right) \tag{C15}$$

As the mass M becomes infinite, an infinite number of capillaries N_{cap} is needed to provide blood to the service volumes. Hence B becomes infinite, as well. Thus, in the limit as $M \to \infty$, the second term in parentheses becomes vanishingly small, and we obtain Kleiber's Law:

$$B \propto M^{\frac{3}{4}} \tag{C16}$$

APPENDIX D: Derivation of the Sigmoid Growth Curve

The WBE ontogenetic growth model partitions metabolic energy use between the energy needed to maintain existing tissue and the energy needed to produce new tissue. The total basal metabolic rate B is the sum of the individual metabolic rates of the body cells, plus the rate at which energy is used to form new cells:

$$B = \sum_c \left[N_c B_c + E_c \frac{dN_c}{dt}\right] \tag{D1}$$

The summation is over the different tissue types within the body. For each tissue type, there are N_c cells, each having a cellular metabolic rate of B_c, with E_c the energy needed to form a new cell for that tissue type. To simplify the analysis, we will treat all N_c of the body's cells as having an average cellular metabolic rate B_c, with E_c being the energy required to create an average body cell:

$$B = N_c B_c + E_c \frac{dN_c}{dt} \tag{D2}$$

The organism's total body mass m is

$$m = m_c N_c \tag{D3}$$

Differentiating both sides of Eq. (D3) with respect to time yields

$$\frac{dm}{dt} = m_c \frac{dN_c}{dt} \tag{D4}$$

Rearranging Eq. (D2) yields

$$\frac{dN_c}{dt} = \frac{1}{E_c}(B - N_c B_c) \tag{D5}$$

Inserting Eq. (D5) into Eq. (D4) yields:

$$\frac{dm}{dt} = \frac{m_c}{E_c}(B - N_c B_c) = \frac{m_c B}{E_c} - \frac{m B_c}{E_c} \tag{D6}$$

Inserting Kleiber's Law, Eq. (2), into Eq. (D6) gives

$$\frac{dm}{dt} = \frac{m_c}{E_c} B_0 m^{\frac{3}{4}} - \frac{m B_c}{E_c} \tag{D7}$$

By defining the taxon-specific parameters *a* and *b* as

$$a \equiv \frac{B_0 m_c}{E_c} \quad b \equiv \frac{B_c}{E_c} \tag{D8}$$

Eq. (D7) simplifies to

$$\frac{dm}{dt} = a m^{\frac{3}{4}} - b m \tag{D9}$$

Growth ceases when the derivative in Eq. (D9) equals 0. This occurs when $m = M$, the mass at maturity, implying that

$$M = \left(\frac{a}{b}\right)^4 = \left(\frac{B_0 m_c}{B_c}\right)^4 \tag{D10}$$

Eq. (D9) thus becomes

$$\frac{dm}{dt} = a m^{\frac{3}{4}} \left[1 - \left(\frac{m}{M}\right)^{\frac{1}{4}}\right] \tag{D11}$$

Separating variables yields

$$\int \left[1 - \left(\frac{m}{M}\right)^{\frac{1}{4}}\right]^{-1} m^{-\frac{3}{4}} dm = a \int dt \tag{D12}$$

Defining

$$u \equiv 1 - \left(\frac{m}{M}\right)^{\frac{1}{4}} \tag{D13}$$

transforms Eq. (D12) into

$$-4M^{\frac{1}{4}} \int \frac{du}{u} = a \int dt, \tag{D14}$$

Integrating and applying the boundary condition that $m(t=0) = m_0$ yields the sigmoid mass-versus-age growth curve:

$$\left(\frac{m}{M}\right)^{1/4} = 1 - \left[1 - \left(\frac{m_0}{M}\right)^{1/4}\right] e^{\frac{-aM^{-1/4}}{4} t} \tag{D15}$$

The age at maturity t_m can be approximated by setting $m = (1-\varepsilon)M$, where $\varepsilon \ll 1$:

$$t_m \approx \left(\frac{4M^{\frac{1}{4}}}{a}\right) ln\left(\frac{4}{\varepsilon}\left[1 - \left(\frac{m_0}{M}\right)^{\frac{1}{4}}\right]\right) \tag{D16}$$

Since $m_0 \ll M$ our expression for t_m simplifies further to

$$t_m \approx \left(\frac{4M^{\frac{1}{4}}}{a}\right) ln\left(\frac{4}{\varepsilon}\right), \tag{D17}$$

which implies that

$$t_m \propto M^{\frac{1}{4}}, \tag{D18}$$

This result is consistent with numerous observations (Lindstedt 1981, Calder 1984, Schmidt-Nielsen 1986) that biological timescales (such as lifespan, blood circulation time, etc.) are generally proportional to $M^{\frac{1}{4}}$. Hence the WBE ontogenetic theory may provide a theoretical link to empirical observations that greater ages at maturity are positively correlated with longer lifespans and adult body masses, and a more fully-developed theory might help explain the great longevity of the pre-Flood patriarchs.

THE AUTHOR

Leo (Jake) Hebert, III earned a B.S. from Lamar University, an M.S. from Texas A&M University, and a Ph.D. (all in physics) from the University of Texas at Dallas. His Ph.D. work examined the possible link between solar activity, cosmic rays, and weather and climate. He has been passionate about creation research since his teenage years. He is a research scientist at the Institute for Creation Research in Dallas, TX, where he has been employed since 2011.